

AFRPL-TR-76-33

12

ADA 030320

**DETERMINATION OF LONG-TERM COMPATIBILITY
OF HYDRAZINE WITH SELECTED MATERIALS OF
CONSTRUCTION**

DESIGN CRITERIA AND GUIDANCE

UNITED TECHNOLOGIES RESEARCH CENTER
EAST HARTFORD, CONNECTICUT 06108

AUTHOR: C.T. BROWN

JUNE 1976

D
REF
SFB
ALL
C

APPROVED FOR PUBLIC RELEASE
DISTRIBUTION UNLIMITED

AIR FORCE ROCKET PROPULSION LABORATORY
DIRECTOR OF SCIENCE AND TECHNOLOGY
AIR FORCE SYSTEMS COMMAND
EDWARDS, CALIFORNIA, 93523

NOTICES

When U. S. Government drawings, specifications, or other data are used for any purpose than a definitely related government procurement operation, the Government thereby incurs no responsibility nor any obligation whatsoever, and the fact that the Government may have formulated, furnished, or in any way supplied the said drawings, specifications or other data, is not to be regarded by implication or otherwise, or in any manner licensing the holder or any other person, or corporation, or conveying any rights or permission to manufacture, use, or sell any patented invention that may in any way be related thereto.

FOREWORD

The work described in this report was performed at the United Technologies Research Center, East Hartford, Connecticut, for the Air Force Rocket Propulsion Laboratory under Contract Fo4611-74-C-0041, ION 305811TP, initiated June 14, 1974 and ending May 15, 1976. Those who participated in the performance of the work under this contract were: Dr. C. T. Brown, Principal Investigator, Mr. D. G. McMahon Program Manager and Chief, Chemical Sciences Section; Ms P.D. DeFelice, Mr. T. L. Fondrk and Mr. J. R. Dannecker.

The work was conducted under the technical management of Lt William Leyden USAF/LKDP and Forrest S. Forbes, Chief Propellant Section.

This report has been reviewed by the Information Office/DOZ and is releasable to the National Technical Information Service (NTIS). At NTIS it will be available to the general public, including foreign nations. This report is unclassified and suitable for general public release.

William Leyden

WILLIAM LEYDEN 2nd Lt. USAF
Project Engineer

Forrest S. Forbes

FORREST S. FORBES, Chief
Propellant Section

FOR THE COMMANDER

Charles E. Sieber

CHARLES E. SIEBER, LTCOL. USAF
CHIEF, LIQUID ROCKET DIVISION

ACCESSION for

NTIS

DOC

UNANNOUNCED

JUSTIFICATION

BY

DATE HIGH/AVAIL

1974 C

E.

A

UNCLASSIFIED

SECURITY CLASSIFICATION OF THIS PAGE (When Data Entered)

19 REPORT DOCUMENTATION PAGE		READ INSTRUCTIONS BEFORE COMPLETING FORM	
1. REPORT NUMBER AFRPL-TR-76-33	2. GOVT ACCESSION NO.	3. RECIPIENT'S CATALOG NUMBER	
4. TITLE (and Subtitle) Determination of Long Term Compatibility of Hydrazine with Selected Materials of Construction		5. TYPE OF REPORT & PERIOD COVERED Design Criteria and Guidance	
7. AUTHOR(s) C. T./Brown		8. CONTRACT OR GRANT NUMBER(s) F04611-74-C-0041	
9. PERFORMING ORGANIZATION NAME AND ADDRESS United Technologies Research Center Silver Lane East Hartford, CT 06108		10. PROGRAM ELEMENT, PROJECT, TASK AREA & WORK UNIT NUMBERS	
11. CONTROLLING OFFICE NAME AND ADDRESS Air Force Rocket Propulsion Laboratory Edwards, CA 93523		12. REPORT DATE June 1976	
14. MONITORING AGENCY NAME & ADDRESS (if different from Controlling Office) Rept. for 14 Jun 74 - 15 May 76		13. NUMBER OF PAGES 61	
16. DISTRIBUTION STATEMENT (of this Report) Approved for Public Release - Distribution Unlimited		15. SECURITY CLASS (of this report) Unclassified	
17. DISTRIBUTION STATEMENT (of the abstract entered in Block 20, if different from Report)		15a. DECLASSIFICATION/DOWNGRADING SCHEDULE	
16. DISTRIBUTION STATEMENT (of this Report) Approved for Public Release - Distribution Unlimited			
16 AF-3058 17 3058 11			
17. DISTRIBUTION STATEMENT (of the abstract entered in Block 20, if different from Report)			
18. SUPPLEMENTARY NOTES			
19. KEY WORDS (Continue on reverse side if necessary and identify by block number) Hydrazine, Material Compatibility, Electrochemical Test Method			
20. ABSTRACT (Continue on reverse side if necessary and identify by block number) An electrochemical accelerated compatibility test method is described. This description includes the theory of the test method, the equipment required to perform the tests and the method for the preparation of the test specimens. A complete step by step experimental procedure is outlined which includes the range of values used for experimental variables such as scan rate, voltage scale, electrolysis current and relaxation time. The			

DD FORM 1 JAN 73 1473 EDITION OF 1 NOV 65 IS OBSOLETE

UNCLASSIFIED

SECURITY CLASSIFICATION OF THIS PAGE (When Data Entered)

409252

LB

determination of metal dissolution and its relationship to hydrazine decomposition rates is discussed.

The results of a series of tests incorporating variables such as metal, metal pretreatment, hydrazine impurities, temperature and time are presented. A statistical analysis of the results using a Graeco-Latin cube design is included which evaluates the relative effect of each of the variables on the value of the equilibrium decomposition current (i_0) ($i_{sub 0}$).

Recommendations for material selection and cleaning and passivation techniques are presented in the light of the experimental results.

SUMMARY

The Design Criteria and Guidance is presented in the form of a handbook which describes the electrochemical accelerated compatibility test method (EAC). In addition the results of a series of tests are given which serve as a guide for material selection and methods for cleaning and passivation of materials which come into contact with hydrazine.

The present report gives a step-by-step procedure for the determination of the equilibrium decomposition current (i_0). This current can be translated into units of mass of hydrazine decomposed per unit surface area per unit time. The optimum operating parameters which yield the most accurate values for i_0 were determined through a series of systematic experiments. These parameters include voltage scan rate and voltage span. The theory of the method is discussed in terms of electron transfer rate control across the metal-solution interface. This type of rate control yields a straight line relationship between the log of the current and the applied potential. The straight line portion of the plot is then extrapolated to zero overpotential to yield the equilibrium current. The translation of this current to the quantitative units mentioned above is based on an understanding of the mechanism of the decomposition reaction. In the case of hydrazine the mechanism is known and involves a four electron transfer for each mole of hydrazine decomposed. This information can then be used in conjunction with Faraday's Law to translate current to quantitative mass units.

The tests are accelerated by means of electrolysis at a current level which is some multiple of i_0 . The ratio of the electrolysis current to i_0 is the acceleration factor. In order to obtain accurate results it is necessary to carefully control the electrolysis current and to allow a sufficient relaxation time after electrolysis prior to the redetermination of i_0 . If the instructions in this report are carried out, it is possible to obtain data up to ten years accelerated time in a period of three to four weeks. This data has been found to compare favorably to real-time results up to four years. The comparison data is presented in this report.

In addition to the test procedure the type of equipment necessary to perform the tests is also described. This equipment consists of a potentiostat used to control the potential between a reference (glass) electrode and the test piece and to supply a current necessary to maintain this potential difference. This current is converted to log form and the log i versus a potential difference is automatically plotted. The change in the potential difference is programmed by means of a motor driven device which changes the potential between the reference electrode and test piece at a prescribed rate over a set voltage range.

The results of a series of 128 tests are presented in which the relative effects of temperature (50, 80, 110, and 160°F) time (0.5, 1.0, 4.0 and 10.0 years) metal pretreatment and impurities (Cl, H₂O, CO₂ and Zn) are independently evaluated. Dissolved metals were also determined and were calculated in terms of the fraction of the total coulombs (ampere-seconds) used for electrolysis that resulted in metal dissolution. In this manner the relative contribution of hydrazine decomposition versus metal dissolution to i_0 can be determined. In most cases, the metal dissolution contribution was less than one percent with the exception of the two aluminum alloys tested (AA1100 and AA6061-T6). The metal dissolution for these alloys was as high as thirty percent in some cases. The remainder of the alloys tested (AM355, 17-7PH, 430 SS, 316L SS, 304L SS and Ti6Al4V) indicated much higher hydrazine decomposition rates than the aluminum alloys in spite of the lower metal dissolution. Of all the metals tested 304L SS and Ti6Al4V were the best in terms of both metal dissolution and hydrazine decomposition. The hydrazine decomposition rates are relatively low and metal dissolution is minimized. 304L SS is self-passivating, but Ti6Al4V requires a special passivating technique for use in hydrazine. It was also found that a special passivation technique for AA1100 prevented pitting corrosion of this alloy, but not for AA6061-T6. However, the latter alloy exhibits the lowest and most consistent hydrazine decomposition rates of all the alloys tested in spite of its susceptibility to pitting corrosion.

It is apparent that further work should be done in the area of surface layers (passivation) and pitting corrosion since there is no metal which does not have a compatibility problem of one type or another. The study reported herein has pinpointed metals that are the best when the parameters, passivation, pitting and hydrazine decomposition are considered. But no single metal has outstanding characteristics in all three areas of compatibility.

TABLE OF CONTENTS

	<u>Page</u>
FOREWORD	i
ABSTRACT	ii
SUMMARY	iv
TABLE OF CONTENTS	vi
SECTION I - INTRODUCTION	1
SECTION II - ELECTROCHEMICAL ACCELERATED COMPATIBILITY TEST METHOD	3
1. Electrochemical Theory	3
2. Experimental Equipment and Test Piece Preparation	7
3. Experimental Test Method	10
4. Metal Dissolution	12
SECTION III - TEST RESULTS	14
1. Preliminary Test Results - Data Comparison	14
2. Basic Test Matrix	16
3. Statistical Analysis	19
SECTION IV - RECOMMENDATIONS FOR MATERIAL SELECTION AND CLEANING AND PASSIVATION TECHNIQUES	22
1. Average Values for i_0	22
2. Degree of Metal Dissolution and Pitting	22
3. Variations in i_0 as a Function of Accelerated Time	23
4. Statistical Analysis	24
5. Conclusions and Recommendations	24
REFERENCES	26
APPENDIX A - DATA REDUCTION METHODS	27
APPENDIX B - METAL PRETREATMENT PROCEDURES	31
APPENDIX C - LIST OF EQUIPMENT	37
TABLES I-IX	38
FIGURES 1-12	47

SECTION I

INTRODUCTION

This handbook is a result of an experimental program, the objective of which was to determine the long-term compatibility of hydrazine and selected materials of construction by means of an electrochemical test method.

The electrochemical test method is based on the fact that the reaction of an electrolyte (hydrazine) on a metal surface can be described in terms of electron transfer. The rate of this electron transfer is measured in the form of an equilibrium current as a function of an applied potential. The mathematics are such that a log current-applied voltage curve is a straight line. When this line is extrapolated to zero applied potential the resulting current is the reaction rate under equilibrium conditions. If the mechanism of the reaction on the surface is known (i.e., hydrazine decomposition) this rate can be translated into quantitative terms such as mass of hydrazine decomposed per unit surface area per unit time.

Once the reaction rate is determined, the time scale for the tests can be condensed by passing a known current (electrolysis) through the electrode (metal) - electrolyte (hydrazine) interface. The ratio of this current and the equilibrium current is the acceleration factor. After the electrolysis has been completed, the process is repeated and the result is a decomposition rate-accelerated time profile of the metal - hydrazine couple.

The test procedure was used to determine the effect of metal, temperature, accelerated time, metal pretreatments and hydrazine impurities for eight metals using a Greaco-Latin Cube statistical procedure. The use of this procedure made it possible to determine the individual contributions of these parameters to the hydrazine decomposition rate while minimizing the number of experiments performed.

In addition, analysis of the metal impurities in solution at the end of each test can be evaluated in terms of the amount of electricity used during the acceleration of the test (i.e., coulombs or ampere-seconds). Using Faraday's law the amount of metal that should have been dissolved during the entire test period (assuming that all the current was involved in metal dissolution) can be compared to the actual dissolved metal concentrations. The ratio of these two values is the fraction of the total current involved in metal dissolution. (The remainder being due to hydrazine decomposition.)

This handbook summarizes the results of the compatibility program in terms of the parameters outlined above. Also included is a complete description of the experimental procedure as well as the equipment required. The data is compared to real time results where possible. Recommendations are made for cleaning and passivation techniques for the alloys tested.

SECTION II

ELECTROCHEMICAL ACCELERATED COMPATIBILITY TEST METHOD

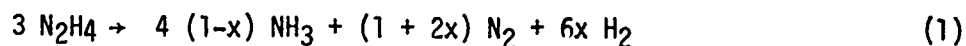
The electrochemical test method is based on the fact that reactions taking place on a metal surface in contact with an electrolyte (in this case the propellant) can be described in terms of electron transfer across the metal-electrolyte interface. The following paragraphs describe the theory of the method as well as the equipment required to perform the experiments and the test conditions to be used to obtain reliable results. The test procedure is outlined in detail.

1. Electrochemical Theory

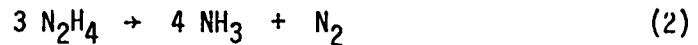
The electrochemical test method has several advantages over other test methods when applied to the measurement of propellant decomposition and metal dissolution in the presence of a propellant. Both these processes can be described in terms of an oxidation-reduction mechanism which implies that some sort of electron transfer is taking place at the metal-propellant interface. The rate of this electron transfer is a measure of propellant decomposition and metal dissolution rates and is directly proportional to current (i.e., electron) flow. It has been determined that the anodic process is controlled by electron transfer while the cathodic process is diffusion controlled. This natural local current flow can be changed by altering the potential energy barrier at the metal-propellant interface using an externally applied potential. The mechanism of the reaction is not changed since the entire process can be accelerated at constant temperature. The rates are specific for those taking place at the metal surface and need not be corrected for decomposition on the container walls (glass) as is the case when gas evolution methods are used.

The electrochemical testing method is based on the fact that any decomposition process on a metal surface is really the sum of two electrochemical processes proceeding at the same rate at the same time. The theoretical basis of the method in terms of both local current flow and the control of the flow by an externally applied potential is described in the following paragraphs for the particular case of hydrazine decomposition.

The overall process for the decomposition of hydrazine can be expressed as:

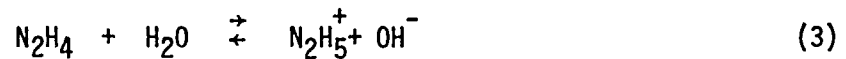


where x represents the fraction of ammonia decomposed. If x is zero, i.e., no ammonia decomposition, the overall reaction is:

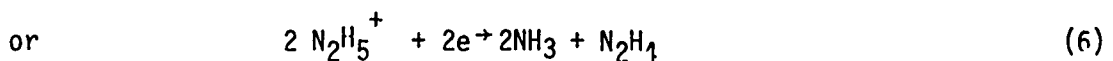
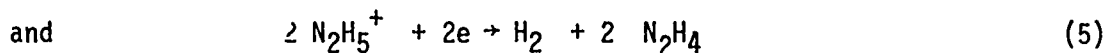
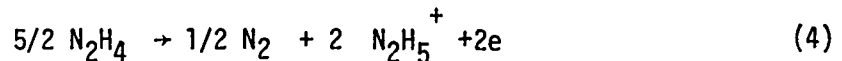


The overall process is really composed of two processes; one, the oxidation of some of the nitrogen in hydrazine to nitrogen gas, and the other the reduction of the remaining nitrogen in hydrazine to ammonia. Any oxidation-reduction process (in this case auto oxidation-reduction) involves the formal transfer of electrons from one species to another. In the presence of a metal the transfer of electrons is accomplished through the metal-liquid interface.

In the presence of small amounts of water (about 0.3 to 0.5 percent in propellant grade hydrazine) a hydrolysis reaction takes place according to:



The N_2H_5^+ (hydrazonium ion) is analogous to the hydrated hydrogen ion in water (H_3O^+) and provides the basis for the electrochemical reactions taking place during hydrazine decomposition. It has been established at UTRC that those reactions are:



The cathodic reaction path appears to be dependent on the metal present. In the presence of platinum the cathodic reaction proceeds exclusively according to Equation 5. In many other cases it is a combination of Equations 5 and 6. Thus one half of the decomposition reaction is expressed by Equation 4, and the other half by Equations 5 and 6 or a combination of the two.

The net current (which is really a measure of the reaction rate) at the metal surface is zero, but partial currents due to Equation 4 and some combination of 5 or 6 are finite. That is:

$$i_{\text{ox}} = |i_{\text{red}}| \quad (7)$$

and
$$i_{\text{ox}} + i_{\text{red}} = 0 \quad (8)$$

where i_{ox} is the partial current due to the oxidation process and i_{red} is that due to the reduction process. The potential (voltage) at the surface as measured against a reference electrode of known potential is called a mixed potential and is the average of the thermodynamic potentials associated with each half reaction (i.e., oxidation and reduction).

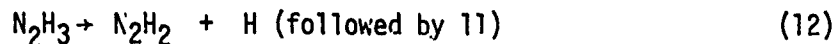
If by some external means, this potential is changed in such a manner as to favor the oxidation or reduction, reaction a net overall current will flow through the system. (A second current-carrying electrode is necessary for this process.) The reference electrode does not carry current, but is used merely as a potential-measuring and control device. Assuming the potential is changed so that the oxidation reaction is favored, i_{ox} will increase and i_{red} will decrease since now:

$$i_{ox} + i_{red} = i_{net} \quad (9)$$

The change in potential from the equilibrium value (known as the overpotential or the polarization) is a linear function of the log of the current if only one electrochemical process (i.e., oxidation) is proceeding on the metal surface. Thus, if the overpotential is plotted versus current on a semilog scale, the plot will be linear at overpotentials high enough to reach the point where i_{ox} is essentially equal to i_{net} (Equation 9). If this were the only process to take place at a particular metal surface, the plot would be linear throughout the entire range of potentials and i_{ox} would be zero at zero overpotential. However, when two processes are taking place at the same metal surface, an extrapolation of the linear portion of the plot would intersect the current axis at a finite current at zero overpotential. This current is i_{ox} under normal conditions when no potential was applied. The same relationship holds true for the measurement of i_{red} .

In the course of the experimental studies it was found that the log i versus ΔE plots had two straight line portions (Fig. 1). In this case, a choice had to be made regarding the portion of the plot to be used which would yield the proper value for i_0 . During the early part of the program the extrapolation was made using the straight line portion of the curve at high overpotential. It was felt that this portion of the curve corresponded to gas (nitrogen) evolution and this was the rate determining step.

Re-examination of the mechanism of hydrazine decomposition based on work published for hydrazine in aqueous solutions (Ref. 1) and work done at UTRC on hydrazine (Ref. 2) indicates that the rate-determining step for hydrazine decomposition occurs at very low overpotentials (200 - 400 mv) and is not dependent on gas formation. Gas formation rates control the process at high overpotentials (> 1.5 volts) but the process of interest in this case is the low overpotential region since it approximates the equilibrium situation. Equations for the anodic decomposition process for hydrazine are shown in Equations 10 through 15. Step 11 is rate controlling, and is repeated four times.



Studies at UTRC (Ref. 2) show that the hydrazone ion (N_2H_5^+) is one of the products of the anodic reaction. This reaction mechanism results in a current-voltage curve, which is a straight line in the low overpotential region indicating activation (electron transfer) control. This line is expressed in terms of the equations:

$$\Delta E = a + b \log i \quad (16)$$

where ΔE is the overpotential and a is the intercept at $E = 0$. The slope, b is expressed as:

$$b = \frac{2.3 RT}{\alpha F} \quad (17)$$

where R is the gas constant expressed in Joules, T is the temperature in $^\circ\text{K}$, F is the Faraday and α is the symmetry factor for the potential energy barrier for electron transfer kinetic control. Equation 17 is for the anodic process only. The cathodic process has a $(1-\alpha)$ terms in the denominator. The intercept (a) contains i_0 , the corrosion or decomposition current at $\Delta E = 0$. The current-voltage relationship (Equation 16) is typical in a process in which the reaction rate is controlled by the transfer of electrons across the metal-solution interface.

This current at zero overpotential (i_0) is equivalent to the rate of reaction of the material in question (i.e., hydrazine). In order to translate this current into the amount of hydrazine decomposed, it is necessary to know the mechanism of the decomposition (i.e., the number of electrons transferred per mole of material decomposed). Since only half the reaction need be measured, the anodic process was chosen because it is straightforward and has been found to obey the current-voltage relationship shown in Equation 16.

The rate of decomposition of hydrazine can thus be determined since four electrons are transferred for each mole of hydrazine decomposed

Equation 11. This corresponds to four Faradays or 385,952 ampere-seconds per mole (i.e., 1.21×10^4 amp sec/gram). This factor, when combined with i_0 in amperes/cm² of surface area, can be used to calculate the rate of hydrazine decomposition in terms of mass/cm²/unit time. Thus, the rate in terms of mg N₂H₄ decomposed/cm²/year would be

$$\text{mg/cm}^2/\text{year} = \frac{i_0 \text{ (amp/cm}^2\text{)}}{1.21 \times 10^4 \text{ amp-sec/mg}} \times 3.1536 \times 10^7 \text{ sec/year} \quad (18)$$

The mg/cm²/year unit can also be translated into rate expressions such as percent decomposed/cm²/10 years or years for 1 percent decomposition/cm². These rate units are summarized in Table I.

2. Experimental Equipment and Test Piece Preparation

The experiments performed, according to the theory outlined above, require special electronic test equipment for the polarization of the metal and the recording of the overpotential versus log current plots as indicated by Equation 16. The following sections of the report describe the preparation of the test specimens, the experimental test cell, the equipment required for the test and the test procedure.

a. Preparation of Test Specimens

The five metals used in the preliminary tests were AA1100, AA6061-T6, AM355, 304L SS and Ti6Al4V. These materials were purchased in either flat plate or bar form. The test specimens were machined from the stock material in the form of a cylinder 0.314 in. diameter and approximately 0.20 in. thick. The diameter was chosen so that the surface area of the test piece would be 0.5 cm². These specimens were then press fit into Teflon holders. These holders are illustrated in Figs. 2 and 3A. Figure 2 is a photograph of a completely assembled test cell. The test pieces fit in a 0.304 in. diameter hole near the bottom of the two cylindrical Teflon holders. Figure 3A is a drawing of a cross section of the test cell showing the position of the test piece (D) in the Teflon holder (C). Prior to the insertion of the test piece, a test piece lead (F) is inserted in an 1/8 in. hole which terminates flush with the bottom surface of the test piece hole. The bottom portion of the lead is flattened and contact is made when the test piece is force fit into place. In instances where the test piece holders had been used several times it was necessary to wrap Teflon tape around the test specimen prior to insertion in order to ensure a leak-tight fit. The test piece lead was also sealed at the top of the test piece holder using a silicone rubber adhesive. This procedure was found to be necessary to prevent liquid from coming into contact with any metal other than the front surface of the test piece. The test piece leads were always the same material as the test piece in order to avoid any potential difference due to a bi-metallic contact.

Once the test piece and holder assembly was completed, the test pieces were ground using 120, 180 and 240 grit silicon carbide paper in successive steps so that a progressively smoother surface is achieved. The final surface is achieved when the test specimen is free of scratches or grooves and has a uniform appearance. Once the grinding has been completed, each test piece is degreased using isopropyl alcohol followed by a deionized water rinse. This procedure is followed by detergent cleaning using liquid detergent in deionized water at 180°F for 5 minutes. The test specimen is then double rinsed with clean deionized water. All the above sample preparation procedures are identical to those specified in the NASA-JPL long-term compatibility test program (Ref. 6).

b. Experimental Test Cell

The experimental test cell, shown in Figs. 2 and 3A, was designed to provide a closed system for the tests using material that would have a minimum interaction with hydrazine. Except for the test specimens, the hydrazine is exposed only to those materials known to be relatively inert. These include pyrex glass, Teflon and ethylene-propylene terpolymer. The glass reference electrode (A) has been found to maintain a stable potential once the glass membrane has been saturated with hydrazine. This potential has been measured with respect to a standard calomel electrode over a long period of time while in contact with hydrazine. The absolute potential of this electrode is not known since the solvent effects on the calomel electrode are uncertain. However as long as a constant potential is maintained, changes in the potential of the test piece with respect to the glass electrode are absolute. Since all voltage measurements are in terms of a ΔE (polarization) an absolute reference potential is not necessary.

Two identical test pieces and test piece holders are used in each cell. Threaded Teflon holders (B) are used for both the test piece and reference electrodes. The test electrode holders and the reference electrode are sealed in the cell by means of ethylene-propylene "O" rings at the base of the threaded Teflon fittings (B). A vent tube (G) is provided for each test electrode compartment. This tube is connected to a Teflon plug stopcock and is vented to a hood.

Drawings of the threaded Teflon caps are shown in Figs. 3B and 3C. They were designed to fit threaded glass fittings from chromatographic columns (Ace Glass - #5820) which include a seat for the "O" ring. The "O" ring sizes are 2-210 for the 25 mm caps (for the test piece holders) and 2-111 for the 15 mm cap (for the glass electrode - ORION #910100 or equivalent). The main sections of the cell are fabricated from 35 mm OD pyrex tubing and are 3.5 inches long as measured from the "O" ring seat. The reference electrode section is fabricated from 20 mm OD pyrex tubing and is 4.0 inches long as measured from the "O" ring seat. The main sections of the cell are joined by means of a short piece (approximately 0.75 in.) of 10 mm OD pyrex tubing to provide for current flow. The three sections of the cell are braced by 5 mm glass rod and are spaced so there is ample room for the three Teflon caps. The two capillary probes from the reference section of the cell are fabricated from 6 mm OD pyrex tubing which are ring-sealed in the walls of the main chambers and which terminate in the

capillary probes (E - Fig. 3A). The probes are positioned so that the tip of the capillary is at the vertical center of the main sections of the cell. Because of the nature of the glass blowing process there is considerable latitude in the exact dimensions of the cell. The only critical considerations are; the position of the capillaries, so that proper spacing is achieved between the capillary tips and the test pieces, and the spacing of the compartments to ensure room for the Teflon caps.

The test piece holder is shown in Fig. 3D. The dimensions are such that the proper spacing can be achieved between the reference capillary and the surface of the test piece. Because of the flexibility of Teflon, it is possible to adjust the spacing by slightly bending the test piece holder. Since there is a minimal current flow between the reference and the test pieces (< one microamp) the only voltage drop in the system is between the tip of the capillary and the test piece. This is the only area in which significant current flow takes place. This voltage drop must be added to the ΔE imposed on the system. However with proper design the voltage drop is minimized to the point where it can be neglected. A series of experiments were performed in which a movable capillary was employed and it was determined that the reference ΔE was minimized with a 2.0 mm outside x 1.0 mm inside diameter capillary placed 2.0 mm from the surface of the test piece. R_{Ω} is defined as the resistance between the test piece and the capillary tip, and was calculated from the equation:

$$R_{\Omega} = \frac{d-0.3 \phi_a}{\chi} \quad (19)$$

where d is the distance between the capillary and the test piece in cm, χ is the specific conductivity of the electrolyte (hydrazine). R_{Ω} is the resulting resistance which causes a potential difference ΔE , provided the ratio of the inside to outside diameter is ≥ 0.5 where ϕ_a is the outside diameter of the capillary. The potential drop (ΔE) is related to the current flow by:

$$\Delta E = i R_{\Omega} \quad (20)$$

Since the specific conductivity of propellant grade hydrazine is approximately $5 \times 10^{-5} \text{ ohm}^{-1} \text{ cm}^{-1}$, $R_{\Omega} \approx 2.8 \times 10^4$ ohms; however, the current levels used are about 10^{-6} amps so $\Delta E = 0.028$ volt. The voltage polarization range for these current levels is about one volt so the 28 mv ΔE is considered to be negligible. It appears that this value could be further reduced by placing the capillary closer to the test piece; however, there is a minimum spacing that can be used before a shielding effect takes place and the actual current flux opposite the capillary is lower than the true current flux on the remainder of the test piece. In general, the distance d , should be greater than the outside diameter of the capillary; however, this distance should be determined experimentally by adjusting the capillary to obtain a ΔE versus d profile. When shielding takes place there will be a much more rapid drop in ΔE versus d than was obtained for a greater value of d .

Two identical test pieces are employed because of the nature of the metal-propellant interaction and also because the tests require that one electrode be polarized anodically and therefore the other must be polarized cathodically. Normal reactions take place at micro-anodic and micro-cathodic sites on the same macro-surface; however, it is necessary to separate these processes when the experiments are performed. Thus, if one test piece is always used as the anode and the other as the cathode, the total products of the reactions during the test should be the same as those on the normal unpolarized surface. This would not be the case if one electrode was the material to be studied and the second electrode was some other inert material such as platinum.

c. Instrumentation

A photograph of the instrumentation required for accelerated compatibility testing is shown in Fig. 4. The central instrument for determining i_0 is a device known as a potentiostat (F). This device is designed to provide a potential difference between the reference and working (test) electrode. A feedback system in the potentiostat provides the current flow necessary to maintain the set potential difference. The potential difference may be set manually, but the standard practice is to automatically scan through a desired potential range at some predetermined rate. For the present application it was desirable to use low scan rates since the kinetics of the process are such that low reaction rates were expected. The potential is scanned by means of a slow sweep programmer (G). The resulting voltage and current signals are fed to an X-Y Recorder (E). The voltage (ΔE) is fed directly to the Y-axis and the current response to the X-axis through a log-converter (D). Plots are made directly on semilog graph paper. The current scale is calibrated by means of a built-in dummy cell incorporating the galvanostic circuits in the particular potentiostat used in this laboratory.

Once the $\log i$ versus ΔE plot is recorded and i_0 is determined, the system under test is electrolyzed using one of the 300 volt constant current power supplies (A). Several constant temperature baths (B) are used in order to run tests at a variety of temperatures simultaneously. Tests performed below room temperature were controlled by means of a Porta-Cool refrigeration unit, while standard thermostatic heaters were used for the elevated temperatures. The specific equipment required is listed in Appendix C.

3. Experimental Test Method

A careful study of the experimental parameters effecting the values of i_0 has been carried out. As a result of this study, which included a statistical analysis of the variable effects at three levels, the following has been determined:

- a) The scan rate used in the potentiostatic polarization must be equal to or less than 50 mv/min. Higher scan rates yield higher values for i_0 . Lower scan rates yield i_0 values identical to those obtained at 50 mv/min.

- b) The polarization range should not exceed two volts, since above this potential nitrogen gas is evolved and the resulting anodic current is sufficient to effect the total decomposition of the hydrazine. It was found that anodic polarization resulted in the most reliable results since the anodic process is electron transfer controlled and thus, results in a linear log i versus voltage plot. This linear plot allows accurate extrapolation to zero applied potential, which corresponds to the equilibrium current (i_0).
- c) The acceleration of the tests was found to yield accurate results provided the electrolysis current was kept to a maximum value of 0.5 ma. This current is sufficient to yield acceleration factors on the order of 1000 since most values of i_0 are low enough that electrolysis currents of about 0.1 or 0.2 ma are sufficient. The lowest value of current for electrolysis should be used which is consistent with reasonable acceleration factors.
- d) The electrolysis time is a minor factor in the reliability of the i_0 values provided it is kept below sixteen to twenty-four hours. Longer electrolysis times yield high results.
- e) The relaxation time is the most important factor in the acceleration portion of the test method. The electrolysis process results in non-equilibrium situations and the equilibration of the system is necessary prior to the redetermination of i_0 . In practice it is convenient to allow the system to equilibrate overnight (approximately sixteen hours). However, in most cases eight hours is sufficient unless the electrolysis current and electrolysis time were used at their maximum values of 0.5 ma and twenty-four hours.

When all the above factors are taken into consideration it should be possible to obtain reliable hydrazine decomposition rate data. In summary, these factors include:

1. Slow voltage sweep rates, (≤ 50 mv/min.) and voltage ranges less than 2.0 volts.
2. Extrapolation of the proper portion of the log i -voltage curve using anodic polarization.
3. Use of electrolysis currents less than 0.5 ma, electrolysis times less than 24 hours, and relaxation times of at least eight hours for the accelerated portion of the test.

The specific experimental procedure is:

- a) The potential between the reference electrode and the test piece (anode) is nulled by means of the potential control on the potentiostat (F - Fig. 4).

- b) The potentiostat is placed in the operate position and the slow sweep scanner (G - Fig. 4) is started. The voltage scale on the slow sweep is set for 2 volts and the scan rate is set for 40 mv/min (i.e., 50 min for 2 volts).
- c) The Y axis on the X-Y Recorder (E - Fig. 4) is set to zero applied potential. The X axis current scale ($\log i$) is precalibrated using a built-in dummy cell. The calibration is set by using the potentiostat in the galvanostatic mode and calibrating at 0.01 and 0.1 ma for two decades of the four cycle semilog graph paper.
- d) The initial current is noted on the graph paper (usually about .0002 ma) and the current- $\log i$ relationship is automatically plotted since the current output of the potentiostat is fed through a log converter.
- e) The extrapolation is made to determine i_0 . This value is then used in conjunction with the desired electrolysis current to determine the acceleration factor for the electrolysis.
- f) The electrolysis is carried out following the restrictions for current and time as outlined above. The positive lead from the power supply is fastened to the test piece; which is always used as the anode. The second test piece is always used as the cathode and is referred to as the counter electrode.
- g) The accelerated time spans are usually set so that shorter periods of time are used during the early part of a test, since the changes in decomposition rate are usually the most pronounced during this time period. The electrolysis experiments for ten year accelerated tests were run so that the accelerated time intervals were 0.25 year for the first two years, 0.5 year for the second two years, 1.0 year for the next three years and 2.0 years for the remainder of the ten years. The electrolysis times varied from 1.5 to 6.0 hours.

When the above procedure is used a plot of hydrazine decomposition rate (i_0) versus accelerated time can be constructed with a minimal amount of data scatter as shown for Ti6Al4V and 304L ss in Figs. 5 and 6, respectively.

4. Metal Dissolution

In addition to the i_0 determination, all the solutions were analyzed for metal impurities at the end of the tests. The dissolved metal data was used to calculate the portion of the total amount of electrical energy passed through the system which was directly attributable to metal dissolution. The total electrical energy measured in coulombs can be related to the amount of material

reacted by use of Faraday's Law which states that one gram-equivalent weight (GEW) of any material will react for every 96,488 coulombs (ampere-seconds). The gram-equivalent weight is the gram-molecular weight (GMW) divided by the number of electrons used for each atom of material. In general, the metal dissolution process can be described by:



where M is the metal in question, M^{+x} is the corresponding metal ion in hydrazine solution, e^{-} is the electron and x is the number of electrons per metal atom dissolved. Calculations were made based on the normal charge for each type of metal ion for each alloy tested. When more than one charge was possible for a given metal ion, the lowest value was used since hydrazine represents a reducing media. For instance, in the case of iron, either Fe^{+2} or Fe^{+3} can exist. For the purpose of this work, Fe^{+2} was chosen and the GEW is the GMW/2. In this manner, the number of coulombs per microgram (μg) of material dissolved can be calculated. This number is based on 100 percent of the current being used for metal dissolution. The ratio of the actual amount of material dissolved to the theoretical value represents the fraction of coulombs associated with metal dissolution. The remainder of the total coulombs are associated with hydrazine decomposition. If this portion of the total i_0 is sufficiently large, the i_0 values for hydrazine decomposition should be corrected accordingly. An example of the calculations for metal dissolution of Ti6Al4V are shown in Table II.

SECTION III

TEST RESULTS

The results for hydrazine decompositions on Ti6Al4V and 304L SS shown in Figs. 5 and 6 were the result of using the values of the experimental parameters shown to yield consistent results. The values for these parameters were the result of the earlier phases of the electrochemical accelerated compatibility (EAC) test method study. In addition to the above metals, AA1100 and AA6061-T6 aluminum alloys and AM355 stainless steel were also investigated.

1. Preliminary Test Results - Data Comparison

The results of the accelerated tests on the five metals studied in the preliminary phase of the test program were compared to real time data where possible. The majority of the real time test data was supplied by NASA-JPL (Refs. 3 and 4). The results of this comparison are shown in Table III.

The decomposition of hydrazine on Ti6Al4V (Fig. 5) increases for about the first two years of accelerated testing time and then levels off to a steady rate of decomposition of about $1.00 \text{ mg/cm}^2/\text{year}$ ($0.1 \times 10^{-3} \text{ ma/cm}^2$ is equivalent to $0.25 \text{ mg/cm}^2/\text{year}$). When this data is compared to that obtained by JPL (Ref. 3) at 2.44, 3.58, and 4.18 real years (Table III) the JPL data is found to be about 30 to 40 percent higher than the UTRC data in two cases and about 10 percent lower in the third case. However, the JPL tests were done with three different test specimens and the variations in their data could be due to variations in the surface of the initial test piece. Although the JPL tests were run for three different periods of time, the variation in the data does not reflect any trend with respect to time. If it is assumed that the variations noted are due to the condition of the test piece surfaces and not time of exposure, then an average value for the hydrazine decomposition rate should be used. The average value for the JPL data is $1.20 \pm .22 \text{ mg/cm}^2/\text{year}$ while the average value for the UTRC data is $1.00 \pm .01 \text{ mg/cm}^2/\text{year}$. Thus, on an average basis for the three JPL test specimens the UTRC and JPL data are in statistical agreement since the range of values for UTRC data (.99 to $1.01 \text{ mg/cm}^2/\text{year}$) falls within the range of values for JPL data (0.98 to $1.42 \text{ mg/cm}^2/\text{year}$.)

The decomposition of hydrazine on 304L stainless steel, in contrast to the Ti6Al4V data, is considerably reduced during the first two years of accelerated testing with a minimum value of about $0.82 \text{ mg/cm}^2/\text{year}$ (Fig. 6). The rate of hydrazine decomposition then rises during the following two years (a total of four years) to about $1.00 \text{ mg/cm}^2/\text{year}$ and stays constant over the period of four to nine years accelerated time. In comparison to the JPL data (Ref. 14) for 1.98 and 2.15 years (Table III) the UTRC data averages $0.829 \pm .01 \text{ mg/cm}^2/\text{year}$ and the JPL data, $0.812 \pm .033 \text{ mg/cm}^2/\text{year}$. Again the agreement is well within statistical error allowing for differences in the two JPL test specimens.

Data comparison with other literature was also accomplished where possible. The results of these comparisons are also summarized in Table III. Data based on gas evolution techniques was obtained several years ago at UTRC for AM355 (Ref. 5). The tests were done at 120°F for a short period of time (72 hours). The electrochemical method was also employed for this alloy, but at 140°F at a minimum time of nine days. Although the rate obtained is about twice the value using gas evolution, the higher temperature could account for most of this difference. It should also be noted that the decomposition rate on AM355 is about an order of magnitude greater than for the other alloys tested and both sets of data reflect this greater rate. Data was also obtained at this time on AA1100 over a period of 72 hours. The electrochemical method for the same time period and temperature (140°F) yields essentially the same rate of hydrazine decomposition. Data for AA6061-T6 was obtained by JPL (Ref. 3) and by Hollywood at JPL (Ref. 4). In the former case the work was done at 110°F and in the latter (using large tanks) the data was obtained over a one month period at 80 to 90°F. In both cases the UTRC data is somewhat higher. The UTRC data indicated a horizontal straight line relationship between decomposition rate and accelerated time over the time period of zero to three years. However, there was some scatter in the data. These data (as well as the AA1100 and AM355 data) were based on the proper extrapolation procedure, (lower part of the log i - ΔE curve) but were not rerun using the optimum values for electrolysis, and relaxation times and electrolysis current as were the Ti6Al4V and 304L SS tests. Thus, any discrepancy between UTRC and literature data is probably due to scatter in the i_0 data.

The above results suggest that the EAC method is a reliable one and can produce long-term compatibility information in a reasonable period of time. In most cases a ten year test can be completed in three to four weeks.

In addition to the decomposition rate data discussed in the preceding paragraphs, the amount of metal dissolution was also determined. In reality i_0 is the sum of the currents involved in metal dissolution and hydrazine decomposition. The relative effects of these two processes are easily determined by means of the EAC test method. The total number of coulombs used for the electrolysis is compared to the amount of material dissolved. The ratio of the coulombs required for the observed metal dissolution to the number of coulombs used is the fraction of i_0 associated with metal dissolution (i.e., electrochemical efficiency for metal dissociation). The extent of metal dissolution and the electrochemical efficiency for metal dissolution was determined using a graphite furnace attachment to the atomic adsorption spectrometer (AAS). This attachment extends the capability of the AAS so that the metal concentrations can be determined in the part per billion range using microliter size samples.

The results of the metal analysis indicate that in the case of Ti6Al4V the highest metal concentrations were associated with a test where there was considerable water contamination. In this case Ti and Al were preferentially dissolved. In the case of 304L SS and AM355, the dissolution of the major metals (Fe, Cr, Ni)

appear to be a direct function of temperature. The same type of behavior is noted in the case of AA1100; however, the amount of Fe, Ni and Cu dissolution is in greater proportion than the concentrations in the alloy. This alloy contains 0.4 percent Fe and 0.2 percent Cu, but only 0.02 percent Ni. The AA6061-T6 alloy contains 0.2 percent Fe, 0.8 percent Mg and 0.4 percent Cu, and 0.02 percent Ni. In this case the Mg was preferentially dissolved as was the iron and nickel.

The fraction of coulombs resulting in metal dissolution for each of the metals was calculated for each test. It was noted that in the case of the titanium alloy and the stainless steels, the coulomb fractions were never greater than 0.13 percent. Thus, 99.87 percent of the current is involved in hydrazine decomposition on the metal surface. However the coulomb fraction for the aluminum alloys is very high in some cases. For AA1100 and AA6061-T6 at 140°F the fraction for aluminum dissolution was about 4 percent in both cases. In other instances, the fractions are about 0.1 to 0.2 percent maximum for the remaining alloy constituents of both AA1100 and AA6061-T6.

The absolute values of i_0 are such that the aluminum alloys yield the lowest values; however, the metal dissolution rates (accompanied by pitting) are the highest. If the effect of dissolved metals (i.e., on a catalyst bed) is of primary importance it appears that the aluminum alloys should be avoided. These observations suggest that both factors should be taken into consideration when materials are being chosen for specific applications.

2. Basic Test Matrix

As a result of the preliminary studies, a test matrix was set up for the study of the relationship of the compatibility of eight metals as a function of temperature, accelerated time, hydrazine impurities and metal pretreatments. The tests were arranged according to the matrix shown in Figs. 7 and 8. The parameters studied are summarized in Table IV. As shown in Figs. 7 and 8, the rows (R) correspond to temperature, the columns (C) to time and the Greek and Latin letters to the metal pretreatments and impurities respectively. Therefore, sixteen tests were run for each of the eight metals for a total of one hundred twenty eight (128) tests. In each set of sixteen tests, no two sets of conditions are the same. The impurity-metal pretreatment combinations are also different for corresponding positions in the matrix for each of the four metals in each group.

The statistical analysis is outlined in detail in Appendix A. By means of this analysis (for each group of four metals) it is possible to independently evaluate the relative effect of all the variables on i_0 .

The experimental apparatus including test cells and instrumentation is identical to that described previously. However, the preparation of the test specimens varied according to the statistical design of the experiments. Pretreatment α (isopropyl alcohol-IPA and detergent) - Table IV, is identical to the cleaning procedure used in the preliminary studies. Pretreatment β was also the same as the previous cleaning procedure except that Trichlor (trichloroethylene) was substituted for IPA. These pretreatments along with special cleaning procedures designated A and B are outlined in Appendix B. They include two different procedures for each base metal type; i.e., titanium, stainless steel and aluminum. The A series are identical to the JPL procedures (JPL Spec No. FS04574 Rev. C, May 1974) (Ref. 6). The B procedures were obtained from other sources (e.g., Modern Electroplating by V. I. Lainer). The impurities were Zn (added as ZnO), 5 ppm; chloride (added as N_2H_5Cl), 20 ppm; CO_2 (added in the vapor phase), 50 ppm; and water, 1.50 percent.

Results for the 128 tests in the two test matrices were obtained in the form of i_0 versus accelerated time plots as well as the analysis of dissolved metals and the fraction of coulombs for metal dissolutions. Details of the results can be obtained from Report AFRPL-TR-76-21. The present report summarizes the i_0 results as a function of the specific parameters outlined in Table IV. The values for i_0 shown in the matrices (Figs. 7 and 8) correspond to the times indicated by T_1 , T_2 , etc. (Table IV). In actual practice i_0 versus accelerated time data were obtained for each test. These plots are significant in many cases since fluctuations in i_0 as a function of time are indicative of the formation and dissolution of passive layers on the test piece surface. This information coupled with metal dissolution data makes it possible to draw a number of conclusions with regard to the compatibility of hydrazine with the metals tested.

In the case of the aluminum alloys, AA1100 and AA6061-T6, the degree of metal dissolution was large compared to the preliminary results in spite of the fact that the total number of coulombs used for electrolysis was much greater in earlier tests compared to the latter tests. The presence of CO_2 and H_2O had the greatest effect on metal dissolution. In most cases, the metal attack was in the form of severe pitting. In the case of AA1100, the B cleaning procedure prevented pitting even though its use resulted in a general etching of the surface. Apparently, localized attack is prevented by avoiding a relatively smooth surface. In the case of AA6061-T6, pitting is also evident, but the result is undissolved metal deposits at the bottom of the test cell. Apparently, the attack is at grain boundaries and the metal is undercut to the point where it disintegrates into fine metal particles. This localized attack is peculiar to the aluminum alloys and these effects deserve further study since the values for i_0 are very low.

The stainless steels AM355, 17-7PH and 430 are all of the same martensitic type. The metal dissolution fractions were low (<1 percent) in most cases, but the values for i_0 were considerably higher than those for the aluminum alloys. The

austenitic stainless steel, 316L also indicated similar results. There were large fluctuations in i_0 versus time which took the form of current reversal indicating the formation and dissolution of a passive layer on the metal surface. The metals of this group were in the order AM355 < 17-7PH < 430 SS < 316L SS in terms of the passive-active behavior. In almost all cases in this series of metals, the B cleaning procedures yielded the highest values for i_0 and the most inconsistent results in terms of metal dissolution. The formation and removal of the passive layer was most evident in the case of 430 SS.

The tests on 304L SS and Ti6Al4V indicate relatively low values of i_0 as well as metal dissolution. The metal dissolution was the lowest for Ti6Al4V. The major dissolving species in this case was iron, a minor constituent for this alloy. There was some pitting and etching, but the majority of cases associated with this phenomena were the result of the B cleaning procedure. When the A cleaning procedure was used, no pitting of any type was noted. The 304L SS indicated metal dissolution (Fe) greater than one percent in some of the one year tests, however this one percent level was noted in tests as large as four years for AM355 and 17-7PH. It appears that the metal dissolution is minimized by the time a one year exposure is achieved and suggests that anodic conditioning could be used to passivate the surface prior to the use of this alloy in practical systems.

The degree of metal dissolution and the fraction of coulombs resulting in metal dissolution is summarized in Tables V and VI for Ti6Al4V and AA1100 respectively. These two alloys represent the best and the worst cases of metal dissolution. It should be noted that the half year tests usually yield abnormally high fractions for metal dissolution. This is probably due to the fact that metal dissolution is more pronounced relative to hydrazine decomposition in a freshly exposed sample. With the exception of the half year tests, the individual metals dissolved from Ti6Al4V were less than one percent except for aluminum in two of the one year tests. The AA1100 tests indicate individual metal dissolution as high as 38 percent for aluminum and about 18 percent for iron.

Pictures of the test pieces for some of the matrix tests are shown in Figs. 9 and 10. The pitting of aluminum is evident in these tests. The etching produced by cleaning procedure B is evident for AM355 and 304L SS. The special case of pitting on Ti6Al4V is illustrated in Fig. 11. This pitting was evident in only a few instances (four tests) and could not be correlated with the test conditions except for the fact that no pitting was evident where cleaning procedure A was used.

In addition to the above tests, a series of experiments were performed on the bi-metallic couples 304L SS/AA6061-T6 and 304L SS/Ti6Al4V. The bi-metallic tests indicated that 304L SS is preferentially dissolved in both cases. It is also observed that i_0 for the two bi-metallic couples is greater than the contribution of each of the individual metals. These tests were performed as a function of time (1.0 and 4.0 years), temperature (110 and 160°F), impurity (Cl and CO₂) and cleaning procedure (IPA-detergent and Trichlor-detergent). The statistical analysis outlined in Appendix A was used to evaluate the effects of the parameters.

The effect on i_0 according to statistical analysis is temperature > bi-metallic couple > impurity. The combination of bi-metallic couple and temperature has the greatest effect. Pictures of the test pieces for two of the eight tests performed are shown in Fig. 12. The pitting of the aluminum is apparent in the one case and a slight etching is noted on Ti6Al4V in the other bi-metallic couple. The major dissolved metals were Fe and Mn in almost all of the tests. The concentration of Al was significant in only one case and Ti was not detected in any of the solutions. In view of these results, it appears that dissimilar alloys should be avoided and stainless steels or aluminum base alloys should be used in pairs for bi-metallic junctions in order to minimize the compatibility problem. The results suggest that the Ti6Al4V / AA6061-T6 couple should have a minimal bi-metallic effect but this should be verified experimentally.

3. Statistical Analysis

The data obtained in the basic test matrix studies were analyzed statistically according to the Graeco-Latin cube design outlined in Appendix A. The final i_0 is the measured response used in the statistical analysis. Because of restrictions on the analysis scheme, each of the sets of four metals is independently treated. In this treatment there must be four values for each of the key variables studied; i.e., four each for time, temperature, pretreatment, impurity and metal.

From the calculation of the analysis of variance for the Graeco-Latin cube, a partitioning of the total sum of squares, the sum of squares for each factor, and the sum of squares of the mean, it is possible to obtain an estimate of the experimental error; i.e., the residual that is not accounted for by the treatment effects. These values are then used to determine the mean squares for each of the variables and the error. The mean square of each variable divided by the experimental error forms the F ratio which is a measure of the significance of each variable as it applies to the measured response (i.e., i_0). As indicated in Appendix A, the sum of squares for each variable is divided by the number of degrees of freedom to obtain the mean square. The degrees of freedom are the number of levels of each variable minus one. The residual mean square is the difference between the total mean square and the mean square accounted for by each variable. If the mean square for a given variable is much greater than the residual mean square, then the effect of this variable on the response is significant. The ratio of the mean square for a given variable to the residual mean square value is called the "F" ratio. The larger the ratio, the greater the effect of the variable on the response; in this case i_0 . The F ratios for the first group of four metals (A1100, AA6061-T6, AM355, and 17-7 PH) were (in descending order); metals, 490.8; temperature, 21.20; time 18.42; impurities, 13.47; and pretreatments, 8.89. It is obvious that the metals themselves had by far the greatest effect on i_0 . However, the relatively low values of i_0 for the aluminum alloys compared to the stainless steels is probably responsible for this effect. For the remainder of the variables, temperature and time had the greatest effect. The effect of the impurities was moderate and the pretreatments had the least effect.

The estimate of the experimental error (σ) for this group of metals is 0.0358×10^{-3} ma/cm² and the grand mean for i_0 (μ) is 0.2673×10^{-3} ma/cm². The individual effects for each level of each variable on i_0 is summarized in Table VII for this metal group. Each value in this table is a measure of the individual effect of each variable at the specified level on the measured response (i.e., i_0). These values can be used to obtain an estimate of the best expected response, by substituting their values into the equation representing the model of the Graeco-Latin cube.

$$Y_{ij}(kl)_m = \mu + R_i + C_j + T_k + G_l + L_m + \epsilon_{ij}(kl)_m \quad (22)$$

where $Y_{ij}(kl)_m$ is the measured response, μ is the true mean response and $\epsilon_{ij}(kl)_m$ is the experimental error. This equation can be used to calculate i_0 for any set of variables including the metal.

The results for the second group of four metals (430 SS, 316L SS, 304L SS, and Ti6Al4V) are summarized in Table VIII. In this case, the grand mean for i_0 (μ) is 0.3925×10^{-3} and the experimental error (σ) is 0.0771×10^{-3} ma/cm². The F ratios are 28.82, 27.89, 16.11, 15.11 and 4.44 for the impurities, pretreatments, temperature, time and metals respectively. It can be seen that the major contributions to i_0 are the pretreatments and impurities, and the metals themselves have very little effect. In this case, three of the four metals were stainless steel.

The F ratios are used to determine the significance of an individual variable with respect to the response; i.e., i_0 . Once it has been determined that the variable is significant, the individual effect of a variable on i_0 for all four metals in a given group (1-4) or (5-8) can be determined by averaging all the responses of all the variables for the four metals. Then, through the use of Equation 22 subtracting out the effects of the other variables, the grand mean and the experimental error. This procedure was used to determine the individual effects in Tables VII and VIII.

An examination of Table VII indicates a regular increase in the time effect for the first group of four metals. The B cleaning procedures have a positive effect on i_0 as does the presence of both CO₂ and H₂O. The temperature effect is not clear since both the highest and lowest values of this variable indicate a positive response while the middle two temperatures indicate a negative response. The response for the metal is not surprising in view of the differences in the aluminum and stainless steel alloys used in this group. For future studies, it would be more advantageous to use alloys with the same base metal for the same test matrix.

The second group of four metals (Table VIII) indicates a fairly regular increase in response with temperature. The time effect is not clear except in the case of the ten year test which yields the highest levels for i_0 , as expected.

The A cleaning procedure had the best effect on i_0 while H_2O and Zn had an adverse effect. The presence of CO_2 appeared to reduce the value of i_0 . The metal effects are more meaningful in this group since three of the four are stainless steels and the titanium alloy does not appear to behave much differently in the presence of hydrazine. The most positive response was obtained with 316L SS and the response was progressively lower for 430 SS, Ti6Al4V and 304L SS in that order.

In terms of hydrazine decomposition, Trichlor and the A cleaning procedures exhibited the most beneficial effect. Of the impurities studied, Cl was the only species that lowered the i_0 values in both sets of metals studied, H_2O was the only species that contributed consistently to higher values for i_0 . Surprisingly CO_2 appeared to have a beneficial effect on the second group of metals. There was also a definite temperature effect for this metal group.

For the first group of four metals (Table VII), the combination of parameters having the largest positive effect on the values of i_0 (i.e., the highest decomposition rate) was AM355 at 10 years and 160°F with the B cleaning procedure and water as an impurity. The combination with the most beneficial effect is AAG061-T6 at four years and 80°F using Trichlor and Joy cleaning as well as chloride as the impurity.

For the second group of four metals (Table VIII), the combination of factors having the most deleterious effect in terms of hydrazine decomposition rate is 316L SS at 10 years and 160°F using IPA and Joy cleaning and H_2O as the impurity. The combination with the most beneficial effect was 304L SS at 0.5 year and 50°F with the A cleaning procedure and CO_2 as the impurity.

The above results are based on the statistical analysis of 128 tests (64 for each combination of four metals). The equation shown previously can be used to predict the best expected response of i_0 for any combination of the five variables evaluated in Tables VII and VIII. It should be noted that only one concentration was used for each impurity and effects of this type should be studied over a concentration range. Also the A and B cleaning procedures (see Appendix B) were not the same in all cases, but were specific for each class of alloy. Taking these limits into account the results of this survey can be used as a guide as to the relative merit of each variable in terms of its effect on the decomposition rate of hydrazine.

SECTION IV

RECOMMENDATIONS FOR MATERIALS SELECTION
AND CLEANING AND PASSIVATION TECHNIQUES

The results of the experimental program are such that a number of factors must be considered in the selection of materials and cleaning and passivation techniques. These factors include the results of the statistical analysis, the degree of metal dissolution, evidence of pitting, the variation of i_0 as a function of accelerated time and the average values of i_0 for each metal.

1. Average Values for i_0

The average i_0 values were used as a relative measure of hydrazine decomposition rate on the metals tested. These average i_0 values are summarized in Table IX, along with the corresponding average hydrazine decomposition rates in mg hydrazine decomposed per cm^2 per year. It is obvious that the aluminum alloys are superior in terms of the average i_0 values. The differences in the i_0 values for the remaining metals are small and range from 0.930 $\text{mg}/\text{cm}^2/\text{year}$ for 304L SS to 1.168 $\text{mg}/\text{cm}^2/\text{year}$ for AM355.

2. Degree of Metal Dissolution and Pitting

In addition to the above comparison, the degree of metal dissolution and/or pitting must be taken into consideration. In this regard, the aluminum alloys were inferior to all the metals tested. In the case of AA1100 it appears that the presence of CO_2 and H_2O accelerated the corrosion. Pitting was severe in most cases except in the case where the B cleaning procedure was used. Although this procedure etches the surface of AA1100, it is the only cleaning procedure tested which prevented pitting. Similar problems of metal dissolution and pitting were evident with AA6061-T6, however, none of the cleaning procedures prevented this type of attack on this alloy.

In the case of the stainless steels of both the martensitic and austenitic types, there was no evidence of metal attack and metal dissolution was minimal. There was a general etching of the metal surfaces when the B cleaning procedure was used. Otherwise, there seemed to be little difference in the use of IPA, Trichlor, or the A cleaning procedure. In general, metal dissolution was greater for 304L SS and 316L SS than for 430 SS, AM355 and 17-7PH.

The titanium alloy (Ti6Al4V) was superior to all the alloys tested in terms of metal dissolution. However, pitting did occur in four tests and an irregular linear etching in two other tests. It was not possible to determine a unifying factor that could explain this phenomena.

In summary, the metal dissolution and pitting were severe for the aluminum alloys, low for the stainless steels, and with the exception of some pitting, very low for Ti6Al4V. The B cleaning procedure eliminated the pitting in the case of AA1100, but caused etching in all other cases.

3. Variations in i_0 as a Function of Accelerated Time

Variations in i_0 as a function of accelerated time can be used as a measure of the stability of protective layers at the metal-solution interface. A lack of variability indicates a stable situation. A gradual rise in i_0 indicates the loss of protection, and conversely a lowering of i_0 as a function of time indicates the formation of a protective layer. Large reversals in the values of i_0 of a cyclic nature indicates a transition state where a protective layer is being alternately formed and dissolved (transpassive behavior).

The aluminum alloys exhibited level, straight line plots of i_0 versus accelerated time. This behavior was particularly pronounced in the case of AA6061-T6 which yielded the most consistent values for i_0 of all the alloys tested.

There were some cyclic reversals in i_0 in the case of AM355, 17-7PH and 430 SS but they were only pronounced in one or two instances for the longer four and ten year tests. The largest effects of this nature were observed with 430 SS and 316L SS where reversals in current were very pronounced. In the case of 316L SS, these reversals resulted in rising values of i_0 as a function of time.

This type of behavior was not observed in the case of 304L SS where the trend for i_0 was downward in most cases except for some of the ten year tests. There were slightly larger fluctuations in i_0 for Ti6Al4V especially for the longer tests, but they were not nearly as pronounced as those for 430 SS and 316L SS.

In terms of these variations some conclusions can be drawn about the long-term compatibility of these metals. For AM355 there are minimal fluctuations. It was also observed that after about one year accelerated time, the observed initial rise in i_0 is reversed indicating self-passivation for this alloy. In the case of 17-7PH and to a greater extent 430 SS and 316L SS, the results indicate unstable surface layers and thus unreliable behavior in terms of hydrazine decomposition. This effect appears to be independent of degree of metal dissolution or contaminants. The 304L SS alloy indicates only slight fluctuations in i_0 but no real reversals in the values of i_0 . Apparently, a stable surface layer is formed. The Trichlor and Joy cleaning procedure is the only treatment that resulted in a consistent downward trend in i_0 as a function of accelerated time for 304L SS. The results for the titanium alloy are less clear but it appears that the A cleaning procedure results in lower and more consistent values for i_0 . The tests in which pitting occurred resulted in the largest fluctuations in i_0 . Evidently Ti6Al4V does not form its own passive layer in contact with hydrazine, and it is necessary to use the A cleaning procedure to protect the surface.

4. Statistical Analysis

The data analysis based on the Graeco-Latin cube design (Tables VII and VIII) indicates a large metal effect for the first metal group (AA1100, AA6061-T6, AM355 and 17-7PH). This effect is colored by the fact that dissimilar base metal alloys were used in this group. When the effects of the other variables are considered, independently of the metals, it is found that the impurities CO_2 and H_2O have a deleterious effect on the compatibility as does the B cleaning procedure. Time has the expected effect (larger times yield greater values of i_0) as does temperature with the exception of the results at 50°F which result in a positive effect on i_0 .

The results for the second group of metals indicate a minimal effect on i_0 for 304L SS followed by Ti6Al4V, 430 SS and 316L SS in increasing order. The B cleaning procedure as well as IPA and detergent yield the highest values of i_0 as does H_2O and Zn as impurities. The highest temperature (160°F) and the longest time (10.0 years) yield the highest values of i_0 , as expected.

5. Conclusions and Recommendations

On the basis of the experimental and statistical results, materials and cleaning procedures must be selected in terms of all the parameters studied. These parameters include the metals themselves, impurities, metal pretreatments, temperature and time. The response to these parameters must include both hydrazine decomposition and metal dissolution. Since temperature and time were only significant at their highest levels (i.e., 160°F and 10.0 years) the effects of cleaning procedures and impurities become more significant. In general, the concentrations of impurities should be minimized, however, it appears that CO_2 and H_2O have the greatest effect on hydrazine decomposition rates. With the impurity levels kept to a minimum, the major factors to be considered are the choice of metal and metal pretreatment which will provide the best balance between hydrazine decomposition rate and metal dissolution and/or pitting.

In terms of low hydrazine decomposition rates, the aluminum alloys should be used. AA6061-T6 is recommended because of its constant behavior as a function of time. However, the metal dissolution and pitting problem must be taken into consideration. In the case of AA1100, it appears that the use of the B cleaning procedure minimizes this problem. However, the nature and causes of aluminum pitting deserves further attention.

In order to minimize problems associated with metal dissolution, it is necessary to use either stainless steels or titanium alloys. Since the absolute values for i_0 are higher for those alloys than aluminum base metals, their selection must be based on minimal metal dissolution coupled with reasonably stable values of i_0 as a function of accelerated time. 316L SS and 430 SS were inferior in this respect. This effect was less pronounced for 17-7PH and AM355, but these alloys exhibited the largest average values for i_0 . Fluctuations in i_0 were significant for 17-7PH, but AM355 tends to form a self-passivating layer. Where

alloys of the martensitic type are called for, it appears that AM355 is desirable in spite of the slightly higher hydrazine decomposition rates associated with its use.

Probably the best compromise between decomposition rate, self-passivation and metal dissolution can be achieved through the use of 304L SS and Ti6Al4V. In the case of 304L SS, fluctuations in i_0 as a function of accelerated time are minimal and this alloy appears to spontaneously form a stable surface layer. Cleaning with Trichlor and detergent is sufficient although cleaning procedure A for 300 series stainless steels also produces a satisfactory surface layer. Ti6Al4V is similar to 304L SS in its compatibility and is also recommended for use in spite of some pitting problems. The use of this metal is not recommended unless the A cleaning procedure for titanium base alloys is used.

In general, the A cleaning procedures are the most satisfactory with the exception of AA1100 where the B cleaning prevented pitting. In most cases, (with the exception of Ti6Al4V) simple solvent-detergent degreasing is sufficient, however, there were no adverse effects noted for any of the A cleaning procedures.

REFERENCES

1. Conway, B. E., N. Mainicic, D. Gilroy, and E. Rudd: Oxide Involvement in Some Anodic Oxidation Reactors. *Journal of the Electrochemical Society*, Vol. 113, No. 11, pp. 1144-1158, November 1966.
2. Brown, C. T.: Electrochemistry of Hydrazine-Hydrazine Azide Mixtures. Presented at the International Conference on "The Properties of Hydrazine and Its Potential Applications as an Energy Source," Poitiers, France, October 1974.
3. Toth, L.: Propellant Material Compatibility, Prepared under NASA Contract NAS7-100, October 1974 (to be published).
4. Hollywood, L. P., et al.: Storage Tests of Nitrogen Tetroxide and Hydrazine in Aluminum Containers. JPL Technical Report 32-1039, January 1967.
5. Rockenfeller, J. D.: Materials Compatibility with Hydrazine-Based Monopropellants. Proceedings of the Tenth Liquid Propulsion Symposium, November 19, 1968, Vol. I, p. 457, CPIA Publication No. 176.
6. "General Cleaning Requirements for Spacecraft Propulsion Systems and Support Equipment". NASA-Jet Propulsion Laboratory, Pasadena, California, JPL Specification FS504574, Rev. C., May 28, 1974.

APPENDIX A
DATA REDUCTION METHODS

Model for Graeco-Latin Cube

The model for this design is

$$Y_{ij(kl)m} = \mu + R_i + C_j + T_k + G_l + L_m + e_{ij(kl)m}$$

$$\left. \begin{array}{l} i \\ j \\ k \\ l \\ m \end{array} \right\} = 1, 2, 3, 4$$

where $Y_{ij(kl)m}$ is the response (i.e., the decomposition of the hydrazine) of the specimen in the i^{th} row, j^{th} column with the k^{th} and l^{th} treatment assignment in the m^{th} layer. μ is the true mean response, and R_i, C_j, T_k, G_l, L_m are the true effects associated with the i^{th} row, j^{th} column, with the k and l treatments in the m^{th} layer. In addition the model assumes that

$$\sum_{i=1}^4 R_i = \sum_{j=1}^4 C_j = \sum_{k=1}^4 T_k = \sum_{l=1}^4 G_l = \sum_{m=1}^4 L_m = 0$$

and the errors $e_{ij(kl)m}$ are independent and normally distributed with mean 0 and variance σ^2 .

The analysis of variance (ANOVA) for this model is shown in Table A-I.

The calculations needed to obtain the Sum of Squares column in the ANOVA are as follows:

The total Sum of Squares, ΣY^2

$$\Sigma Y^2 = \left(\sum_{j=1}^4 \sum_{k=1}^4 \sum_{l=1}^4 Y_{ij(kl)m}^2 \right) / 4^3$$

i.e., the measured response of all the specimens tested are squared and summed and then divided by the total number of degrees of freedom (i.e., the number of specimens used to form the cube, $4 \times 4 \times 4 = 64$).

The Sum of Squares due to the Mean, M_{yy}

$$M_{yy} = \left(\sum_{j=1}^4 \sum_{k=1}^4 \sum_{m=1}^4 Y_{ij(kl)m} \right)^2 / 4^3$$

i.e., the grand sum of the measured responses of all the tested specimens represented by the matrix elements is squared and divided by the total number of degrees of freedom.

The Row Sum of Squares, R_{yy} (temperatures)

$$R_{yy} = \left(\sum_{j=1}^4 \sum_{m=1}^4 R_{im}^2 \right) / 4^2 - M_{yy}$$

i.e., the row totals are squared and summed and then divided by the number of rows for the four matrices, and are corrected for mean square by subtracting M_{yy} .

The Column Sum of Squares, C_{yy} (time)

$$C_{yy} = \left(\sum_{j=1}^4 \sum_{m=1}^4 C_{im}^2 \right) / 4^2 - M_{yy}$$

i.e., the column totals are squared and summed and then divided by the number of columns for the four matrices, and are corrected for mean square by subtraction, M_{yy} .

The Treatment Sum of Squares, T_{yy} (Latin Letters) - Impurities

$$T_{yy} = \left(\sum_{k=1}^4 \sum_{m=1}^4 T_{km}^2 \right) / 4^2 - M_{yy}$$

i.e., the treatment totals (impurities) are squared and summed and then divided by the number of treatments for the four matrices, and are corrected for the mean square by subtracting, M_{yy} .

The Treatment Sum of Squares, G_{yy} (Greek Letters) - Pretreatment

$$G_{yy} = \left(\sum_{l=1}^4 \sum_{m=1}^4 G_{lm}^2 \right) / 4^2 - M_{yy}$$

i.e., the treatment totals (metal pretreatments) are squared and summed and then divided by the number of columns for the four matrices, and are corrected for mean square by subtracting M_{yy} .

The Layers Sum of Squares, L_{yy} (materials)

$$L_{yy} = \sum_{m=1}^4 \left(\sum_{j=1}^4 \sum_{i=1}^4 Y_{ij} \right)^2 / 4 - M_{yy}$$

i.e., the total sum of observations for each matrix is squared and summed over the four matrices. This total is then divided by 4 and corrected for mean square by subtracting M_{yy} .

The Experimental Error Sum of Squares, E_{yy}

$$E_{yy} = \sum Y^2 - M_{yy} - R_{yy} - C_{yy} - T_{yy} - G_{yy} - L_{yy}$$

The experimental error sum of squares is obtained by subtracting the sum of squares due to the mean, rows, columns, 2 treatments and the layers. It represents that part of the variation that is not accounted for by the treatment effects, column and row and layer effects. Where E_{yy} is divided by 4^3 we obtain an estimate for σ^2 , the experimental error. With this, one can perform the necessary statistical tests to determine whether or not the treatment effects are significant.

Table A-I illustrates the format for the statistical analysis where the mean square for each variable and the residual (error) are calculated from the sum of squares. The ratio of the response of each variable to the residual is the F ratio which is a measure of the relative effect of each variable to the response, in this case, i_0 .

TABLE A-I
ANOVA-GRAECO-LATIN CUBE

(one observation per experimental unit)

Source of Variation	Degrees of Freedom	Sum of Squares	Mean Square	F-Ratio
MEAN----	1	M_{yy}	$M = M_{yy}/1$	
ROWS---- (Temperature)	3	R_{yy}	$R = R_{yy}/3$	R/E
COLUMNS---- (Time)	3	C_{yy}	$C = C_{yy}/3$	C/E
LATIN LETTERS---- (Impurities)	3	T_{yy}	$T = T_{yy}/3$	T/E
GREEK LETTERS---- (Metal Pretreat)	3	G_{yy}	$G = G_{yy}/3$	G/E
LAYERS---- (Materials)	3	L_{yy}	$L = L_{yy}/3$	L/E
ERRORS----	48	E_{yy}	$E = E_{yy}/48$	
TOTAL	64	ΣY^2		

APPENDIX B
METAL PRETREATMENT PROCEDURES

Titanium A

Step	Solution	Temp (°F)	Time (minutes)
1.	Degrease with Isopropyl Alcohol (IPA)	Ambient	5-10 sonic
2.	Rinse with H ₂ O distilled sonic (performed twice)	Ambient	Until pH within 0.2 of source
3.	Alkaline Oakite, 3% by volume	170 ± 10	5-10
4.	Repeat Step (2.)		
5.	Acid HNO ₃ , 45% by volume	75 ± 10	20-30
6.	Rinse H ₂ O distilled	Ambient	
7.	Repeat Step (2.)		
8.	Detergent Cleaning, 1% solution by volume	170 ± 20	5-10
9.	Repeat Step (2.)		
10.	Final Rinse - H ₂ O, deionized	Ambient	As necessary to achieve desired particulate level
11.	Dry - Purge H ₂	Ambient	
12.	Dry-vacuum	120 ± 10	60
13.	Dry-vacuum	Ambient	

. 300 Steel - A

300 Series SS (304L, 316L)

Step	Solution	Temp (°F)	Time (minutes)
1.	Degrease Isopropyl Alcohol (IPA)	Ambient	5-10 Sonic, 30-60 Hand Agitate
2.	Rinse - H ₂ O, distilled, Sonic (performed twice)	Ambient	Until pH within 0.2 of source
3.	Alkaline Oakite, 3% by volume	170 ± 10	5-10
4.	Repeat Step (2.)		
5.	Acid HNO ₃ , 10% by volume	75 ± 10	10-15
6.	Rinse H ₂ O distilled	Ambient	
7.	Repeat Step (2.)		
8.	Detergent Clean, 1% solution by volume	170 ± 20	5-10
9.	Repeat Step (2.)		
10.	Final Rinse - IPA	Ambient	As necessary to achieve desired particulate level
11.	Dry-Purge N ₂	Ambient	Filtered-dew point must be drier than internal source
12.	Dry-vacuum	120 ± 10	1.0
13.	Dry-vacuum	Ambient	

400 Steel - A

Precip. Hard SS + 400 Series SS
(17-7PH, AM355, 430)

Step	Solution	Temp (°F)	Time (minutes)
1.	Degrease Isopropyl Alcohol (IPA)	Ambient	5-10 Sonic, 30-60 Hand Agitate
2.	Rinse - H ₂ O, distilled, sonic (performed twice)	Ambient	Until pH within 0.2 of source
3.	Alkaline Oakite, 3% by volume	170 ± 10	5-10
4.	Repeat Step (2.)		
5.	21% HNO ₃ + 22 Grams/liter Sodium Dichromate	75 ± 15	10-15
6.	Rinse H ₂ O distilled	Ambient	
7.	Repeat Step (2.)		
8.	Detergent Clean, 1% solution by volume	170 ± 20	5-10
9.	Repeat Step (2.)		
10.	Final Rinse IPA	Ambient	As necessary to achieve desired particulate level
11.	Dry-Purge N ₂	Ambient	Filtered-dew point must be dried than internal source
12.	Dry-vacuum	120 ± 10	1.0
13.	Dry-vacuum	Ambient	

Aluminum - A

Step	Solution	Temp (°F)	Time (minutes)
1.	Degrease Isopropyl Alcohol (IPA)	Ambient	5-10 Sonic
2.	Rinse - H ₂ O distilled, sonic (performed twice)	Ambient	Until pH within 0.2 of source
3.	Alkaline Oakite, 3% by volume	150 ± 10	10-15
4.	Repeat Step (2.)		
5.	Detergent clean, 19% solution by volume	70 ± 20	5-10
6.	Repeat Step (2.)		
7.	Final Rinse - IPA	Ambient	As necessary to achieve desired particulate level
8.	Dry-Purge H ₂	Ambient	Filtered-dew point must be drier than internal source
9.	Dry-vacuum	120 ± 10	1.0
10.	Dry-vacuum	Ambient	

Aluminum - B

1.	Degrease		
2.	5 oz/gal Na ₃ PO ₄ -H ₂ O	180-200	1-3
3.	Rinse dist. H ₂ O		
4.	1% HF, 1% HNO ₃ -H ₂ O	Rm Temp	1
5.	Rinse distilled H ₂ O		
6.	Dry		

Titanium - B

Step	Solution	Temp (°F)	Time (minutes)
1.	Abrasive clean (Ajax, Babo) (Scrub by hand)	Ambient	
2.	Rinse - deionized H ₂ O	Ambient	Until pH within 0.2 of source
3.	Pickling: HNO ₃ - 20% HF - 5% Balance, H ₂ O	Ambient	15-30 seconds
4.	Rinse - deionized H ₂ O	Ambient	Until pH within 0.2 of source
5.	Anodic Etch Glacial acetic acid - 87.5% HF - 12.5% 20 ma/cm ²	Ambient	30
6.	Final Rinse - deionized H ₂ O	Ambient	Until pH within 0.2 of source
7.	Dry-Purge N ₂	Ambient	

Stainless Steel - B

Series 300 and 400

Step	Solution	Temp (°F)	Time (minutes)
1.	Degrease NaOH, 25 g/l Na ₃ PO ₄ , 25 g/l Na ₂ SiO ₃ , 5 g/l	70-90°C	10-30
2.	Rinse - deionized H ₂ O	Ambient	Until pH within 0.2 of source
3.	Pickling: HCl - 25% HNO ₃ - 5% Inhibitor - 0.5% Balance - H ₂ O	60-70°C	10-20
4.	Final Rinse - deionized H ₂ O	Ambient	Until pH within 0.2 of source
5.	Dry-Purge N ₂	Ambient	

APPENDIX C

LIST OF EQUIPMENT

I. Electronic Apparatus

- a) Potentiostat-Galvanostat, PAR Model 173 or Equivalent
- b) Logarithmic Current Converter (Either PAR Model 376, Hewlett-Packard Model 7562A or Equivalent)
- c) X-Y Recorder, Mosley Model 135 AM or Equivalent
- d) Automatic Baseline Advance, Elscint Model ABA-26 or Equivalent
- e) Power Supplies - Kepco Model PC-2 (Constant Current) (100v-200 ma max.) or Electronic Measurements Model C612 (300v-100 ma max.) or Equivalent

II. Constant Temperature Apparatus

- a) Heating and Control - Precision Scientific Porta-Temp or Equivalent
- b) Cooling and Control - Precision Scientific Porta-Cool or Equivalent

TABLE I

CALCULATIONS FOR N_2H_4 DECOMPOSITIONElectrochemical Equivalents:

4 Faradays/mole hydrazine decomposed
 or 8 grams/Faraday
 or 1.21×10^4 ampere-sec/gram

I. Weight of hydrazine decomposed/cm²/sec or cm²/year

$$g N_2H_4/cm^2/sec = \frac{i_o(\text{amp/cm}^2)}{1.21 \times 10^4 \text{ amp-sec/g}}$$

$$\text{or } mg N_2H_4/cm^2/year = \frac{i_o(\text{amp/cm}^2)}{1.21 \times 10^1 \text{ amp-sec/mg}} \times 3.1536 \times 10^7 \text{ sec/year}$$

II. Hydrazine decomposition in terms of percent decomposed in 10 years/cm²

$$\% \text{ decomposed/cm}^2/10 \text{ years} = \frac{mg/cm^2/year}{g N_2H_4}$$

III. Time in years for 1.0% decomposition/cm²

$$\text{years for 1.0\% decomposition/cm}^2 = \frac{1\%}{\% \text{ decomposition in 10 years}} \times 10$$

TABLE II
METAL DISSOLUTION IN HYDRAZINE
(Ti6Al4V)

Temperature (°F)	No. of Coulombs	µg Metals in Solution			Fraction of Coulombs Resulting in Metal Dissolution			
		Ti	Al	Ni	Ti (x 10 ⁴)	Al (x 10 ⁴)	Fe (x 10 ⁴)	Ni (x 10 ⁴)
140	623.95	.068	--	94.09	8.45	.0044	5.22	.447
110	89.67	.138	2.42	34.61	3.53	.062	13.35	1.30
50	4422.72	40.67	114.89	12.20	6.30	.371	.095	.047

TABLE III

COMPARISON OF UTRC
AND LITERATURE DATA(mg/cm²/yr)

<u>Material</u>	<u>Temperature</u> (°F)	<u>Time</u> (Years)	<u>UTRC</u> <u>Gas Evolution</u> (Ref 13)	<u>JPL</u> (Ref 14)	<u>JPL</u> (Ref 15)	<u>UTRC</u> <u>Electrochemical</u> <u>Data</u>
AM355	120	.0082	11.29	--	--	--
AM355	140	.025*	--	--	--	25.33
AA1100	140	.0082	1.17	--	--	1.42
304L SS	110	1.98	--	.847	--	.823
304L SS	110	2.15	--	.780	--	.828
Ti6Al4V	110	2.44	--	1.42	--	.998
Ti6Al4V	110	3.58	--	.883	--	1.01
Ti6Al4V	110	4.18	--	1.31	--	1.04
AA6061-T6	80-90	.082	--	--	.77	--
AA6061-T6	110	.082	--	--	--	.811
AA6061-T6	110	3.18	--	.422	--	.811

*Was in test nine (9) days before first scan (i_0) was taken.

TABLE IV
 GRAECO-LATIN CUBE
 (Test Conditions)

Rows - Temperatures

$R_1 = 50^\circ$

$R_2 = 80^\circ$

$R_3 = 110^\circ$

$R_4 = 160^\circ$

Columns - Times

$T_1 = 6 \text{ months}$

$T_2 = 1 \text{ year}$

$T_3 = 4 \text{ years}$

$T_4 = 10 \text{ years}$

Latin Letters - Impurities

$A = \text{CO}_2$

$B = \text{Cl}$

$C = \text{H}_2\text{O}$

$D = \text{Zn}$

Greek Letters - Metal Pretreatments

$\alpha = \text{IPA} + \text{Detergent}$

$\beta = \text{Trichlor} + \text{Detergent}$

$\gamma = \text{A}$

$\delta = \text{B}$

Layers - Materials (Group I)

1 - AA1100

2 - AA6061-T6

3 - AM355

4 - 17-7PH

Layers - Materials (Group II)

5 - 430 SS

6 - 316L SS

7 - 304L SS

8 - Ti6Al4V

TABLE V
METAL DISSOLUTION IN HYDRAZINE
(Ti6Al4V)

Test No.	Temperature (°F)	Time (Years)	No. of Coulombs	µg Metal in Solution				Fraction of Coulombs Resulting in Metal Dissolution					
				Ti	Al	V	Fe	Ni	Ti	Al	V	Fe	Ni
1	50	0.5	2.578	1.627	3.660	1.627	10.574	26.841	.00255	.0154	.00240	.0142	.0343
2	50	1.0	5.590	2.440	4.067	2.440	6.507	2.440	.00176	.00790	.00166	.00403	.00144
3	50	4.0	15.655	18.707	2.033	1.220	36.601	4.067	.00481	.00141	.00030	.09809	.00086
4	50	10.0	60.197	58.562	24.401	1.301	8.134	-	.00392	.00440	.00008	.00047	-
5	80	0.5	4.281	11.306	25.036	1.373	26.651	29.881	.0106	.0179	.00121	.0215	.0230
* 6	.50	1.0	6.096	4.067	6.100	2.440	4.880	-	.00269	.0108	.00152	.00277	-
7	80	4.0	25.082	4.846	5.249	1.777	9.691	-	.00078	.00227	.00027	.00134	-
8	80	10.0	76.366	2.423	2.584	-	13.729	-	.00013	.00037	-	.00062	-
9	110	0.5	1.155	1.582	1.978	1.107	18.985	-	.00550	.0187	.00365	.0569	-
10	110	1.0	4.975	1.582	3.164	-	42.716	9.492	.00128	.00690	-	.0297	.00628
11	110	4.0	30.660	13.448	18.985	-	4.746	-	.00176	.00672	-	.00054	-
12	110	10.0	66.752	7.119	7.910	1.424	7.910	-	.00043	.00128	.00008	.00041	-
13	160	0.5	.690	3.087	3.473	-	8.490	-	.0181	.0546	-	.0427	-
14	160	1.0	8.155	3.087	7.718	1.080	20.068	6.638	.00153	.0103	.00050	.00853	.00268
15	160	4.0	6.736	2.316	3.087	-	39.364	-	.00139	.00498	-	.0202	-
16	160	10.0	94.590	.772	3.087	1.080	6.946	-	.00003	.00035	.00004	.00025	-

* Test No. 6 was inadvertently run at 50°F instead of 80°F

TABLE VI

METAL DISSOLUTION IN HYDRAZINE
(AAL100)

Test No.	Temperature (°F)	Time (Years)	No. of Coulombs	µg Metal in Solution			Fraction of Coulombs Resulting in Metal Dissolution		
				Al	Fe	Cu	Al	Fe	Cu
1	50	.528	.9374	5.33	19.0	.76	.061	.070	.0025
2	50	1.04	1.661	10.5	16.2	.81	.069	.033	.0015
3	50	1.35	2.518	7.62	4.57	1.14	.032	.006	.0014
4	50	10.0	15.311	62.5	9.1	.762	.044	.002	.00015
5	80	.522	.7458	10.5	18.0	.751	.153	.083	.0031
6	80	1.05	1.614	7.21	64.1	2.00	.048	.137	.0038
7	80	4.08	8.950	8.01	88.1	12.02	.010	.034	.0041
8	80	.671	.6057	5.61	31.2	--	.10	.178	.0040
9	110	.849	1.882	34.1	1040.0	3.33	.19	1.90	.0055
10	110	1.01	2.250	48.2	26.8	1.42	.23	.0414	.0019
11	110	4.06	12.844	129.0	185.0	10.3	.10	.049	.0025
12	110	10.01	16.254	577.0	174.0	11.8	.38	.037	.0022
13	160	.510	.5984	69.0	108.0	34.0	1.25	.627	.17
14	160	1.07	2.423	73.3	123.0	8.49	.328	.176	.010
15	160	2.26	4.287	49.3	7.71	--	.125	.006	.0006
16	160	1.06	2.917	27.0	57.8	27.7	.100	.068	.029

TABLE VII
 GRAECO-LATIN CUBE
 ESTIMATE OF EFFECTS

<u>Rows</u>	<u>Temperatures</u> (°F)	<u>Response</u> (i_0^*)	<u>Columns</u>	<u>Time</u> (Years)	<u>Response</u> (i_0^*)
\hat{R}_1	50	+0.0158	\hat{C}_1	0.5	-0.0073
\hat{R}_2	80	-0.0206	\hat{C}_2	1.0	-0.0054
\hat{R}_3	110	-0.0126	\hat{C}_3	4.0	-0.0104
\hat{R}_4	160	+0.0173	\hat{C}_4	10.0	+0.0231

<u>Latin</u>	<u>Impurities</u>	<u>Response</u> (i_0^*)	<u>Greek</u>	<u>Pretreatments</u>	<u>Response</u> (i_0^*)
\hat{A}	CO ₂	+0.0124	$\overset{\wedge}{\alpha}$	IPA and Joy	-0.0038
\hat{B}	Cl	-0.0159	$\overset{\wedge}{\beta}$	Trichlor and Joy	-0.0088
\hat{C}	H ₂ O	+0.0130	$\overset{\wedge}{\gamma}$	A	-0.0048
\hat{D}	Zn	-0.0094	$\overset{\wedge}{\delta}$	B	+0.0172

<u>Layers</u>	<u>Metals</u>	<u>Response</u> (i_0^*)
\hat{L}_1	AAl100	-0.1494
\hat{L}_2	AA6061-T6	-0.1932
\hat{L}_3	AM355	+0.1805
\hat{L}_4	17-7PH	+0.1620

*Each value refers to i_0 in $\text{ma/cm}^2 \times 10^{-3}$

TABLE VIII

 GRAECO-LATIN CUBE
 ESTIMATE OF EFFECTS

<u>Rows</u>	<u>Temperatures</u> (°F)	<u>Response</u> (i_0^*)	<u>Columns</u>	<u>Time</u> (Years)	<u>Response</u> (i_0^*)
\hat{R}_1	50	-0.0406	\hat{C}_1	0.5	-0.0594
\hat{R}_2	80	-0.0053	\hat{C}_2	1.0	+0.0200
\hat{R}_3	110	-0.0094	\hat{C}_3	4.0	-0.0094
\hat{R}_4	160	+0.0682	\hat{C}_4	10.0	+0.0620

<u>Latin</u>	<u>Impurities</u>	<u>Response</u> (i_0^*)	<u>Greek</u>	<u>Pretreatments</u>	<u>Response</u> (i_0^*)
\hat{A}	CO ₂	-0.0834	$\overset{\wedge}{\alpha}$	IPA and Joy	+0.0841
\hat{B}	Cl	-0.0025	$\overset{\wedge}{\beta}$	Trichlor and Joy	-0.0084
\hat{C}	H ₂ O	+0.0544	$\overset{\wedge}{\gamma}$	A	-0.0744
\hat{D}	Zn	+0.0444	$\overset{\wedge}{\delta}$	B	+0.0172

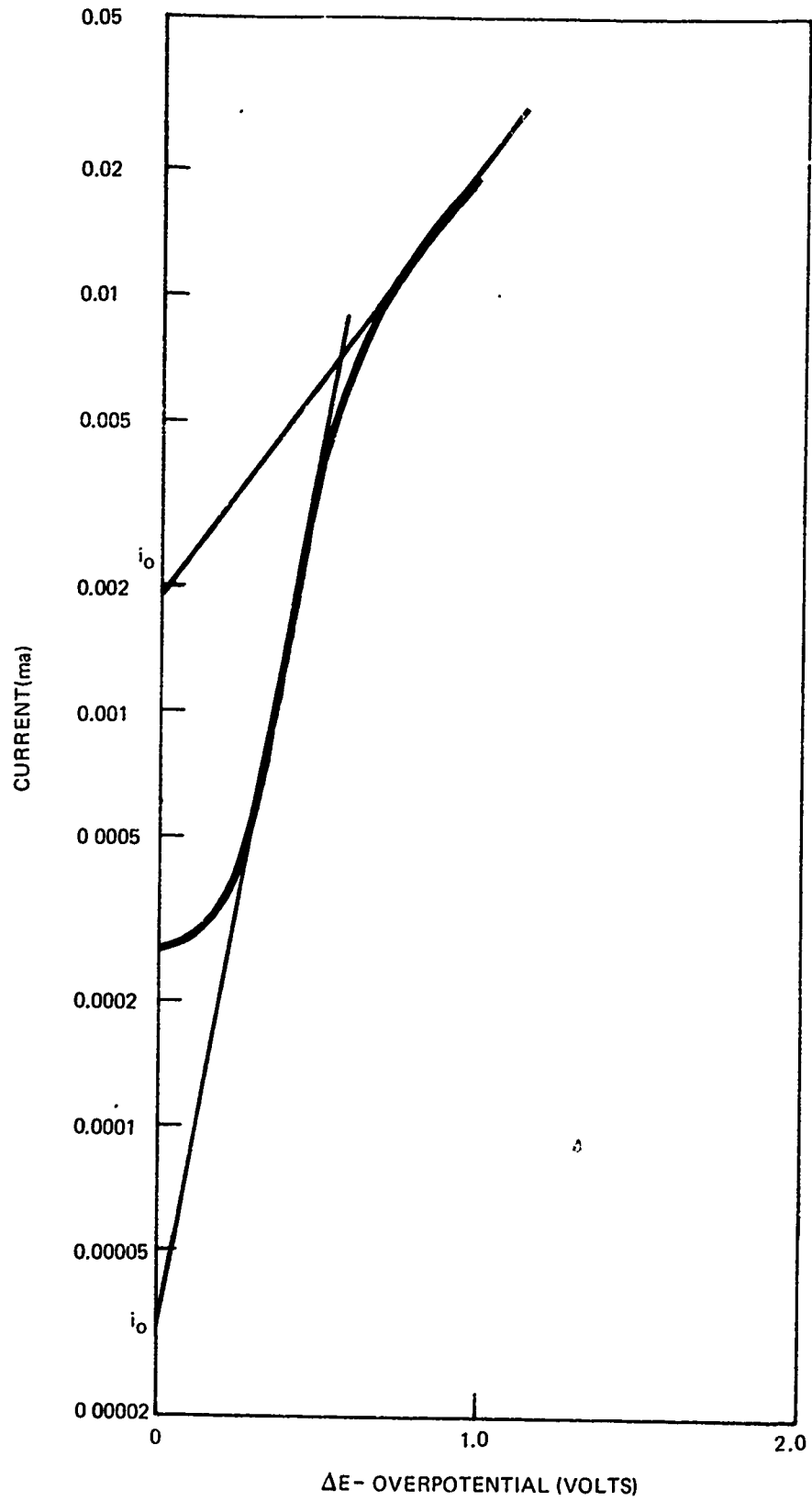
<u>Layers</u>	<u>Metals</u>	<u>Response</u> (i_0^*)
\hat{L}_5	430 SS	+0.0181
\hat{L}_6	316L SS	+0.0406
\hat{L}_7	304L SS	-0.0484
\hat{L}_8	Ti6Al4V	-0.0100

*Each value refers to i_0 in $\text{ma}/\text{cm}^2 \times 10^{-3}$

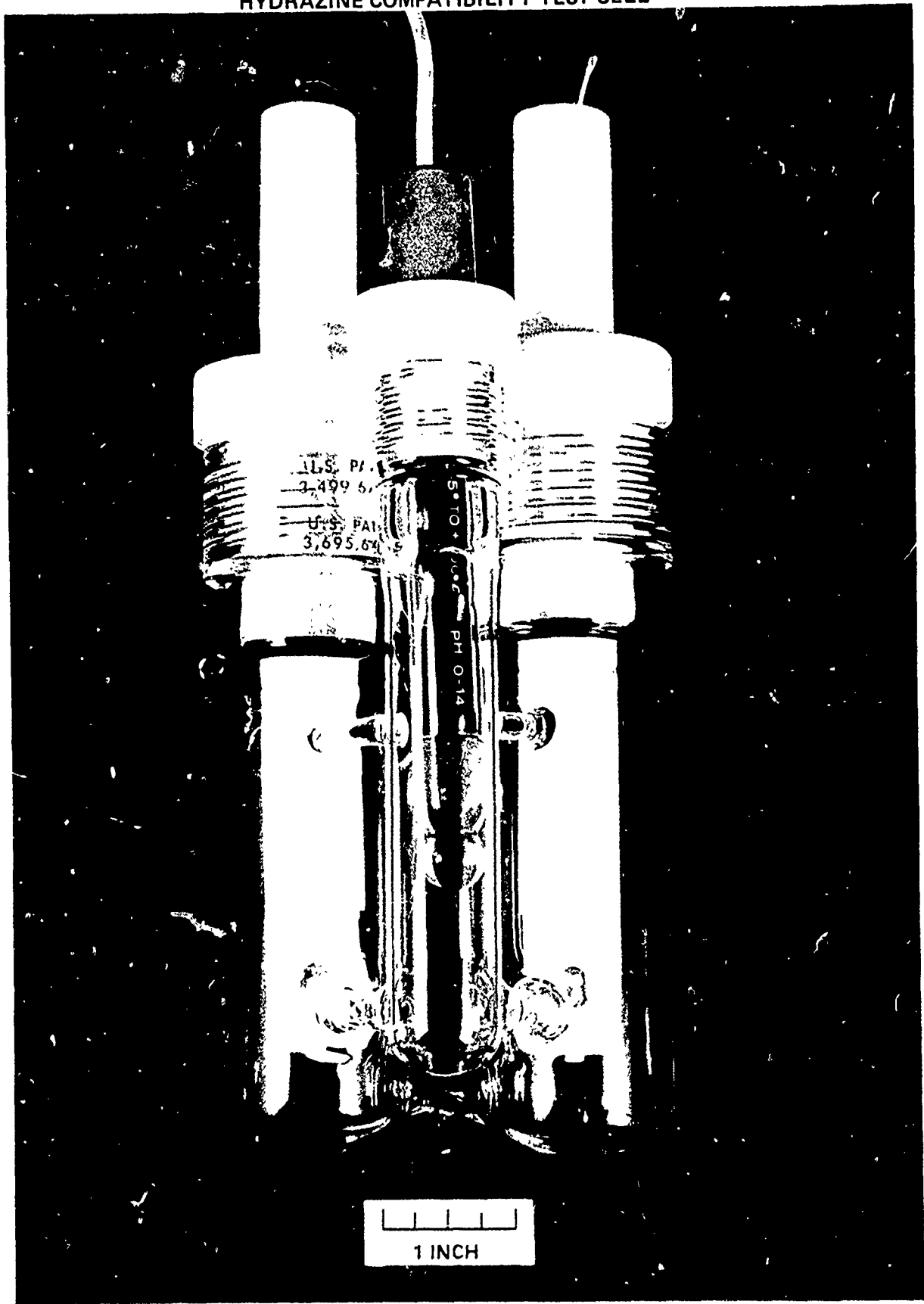
TABLE IX
AVERAGE DECOMPOSITION RATES

<u>METAL</u>	<u>Average i_o (ma/cm^2)$\times 10^3$</u>	<u>Average Decomposition Rate ($\text{mg}/\text{cm}^2/\text{year}$)</u>
AA6061-T6	0.074	0.193
AA1100	0.118	0.308
304L	0.357	0.930
Ti6Al4V	0.382	0.996
430 SS	0.411	1.071
316 SS	0.427	1.113
17-7PH	0.429	1.118
AM355	0.448	1.168

POTENTIOSTATIC LOG CURRENT-VOLTAGE RELATIONS FOR ANHYDROUS HYDRAZINE

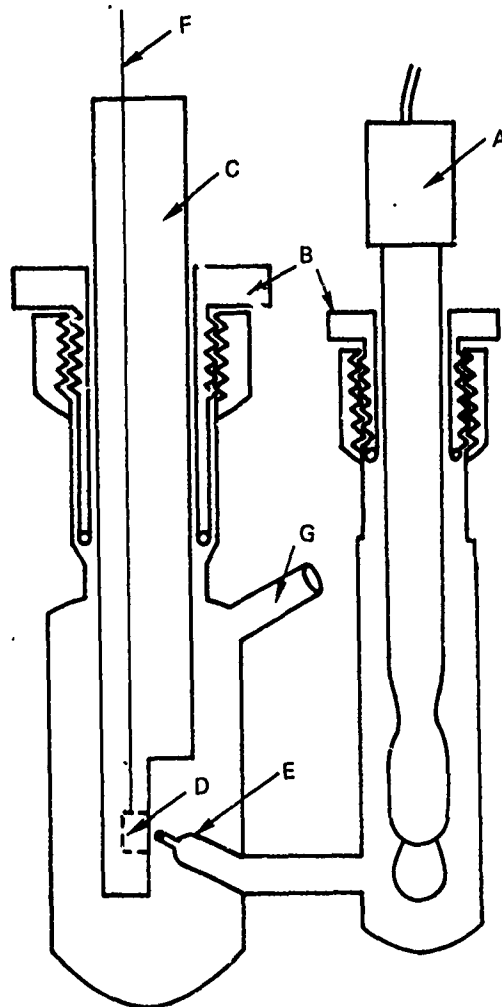


HYDRAZINE COMPATIBILITY TEST CELL



HYDRAZINE COMPATIBILITY TEST CELL

(CROSS SECTION)

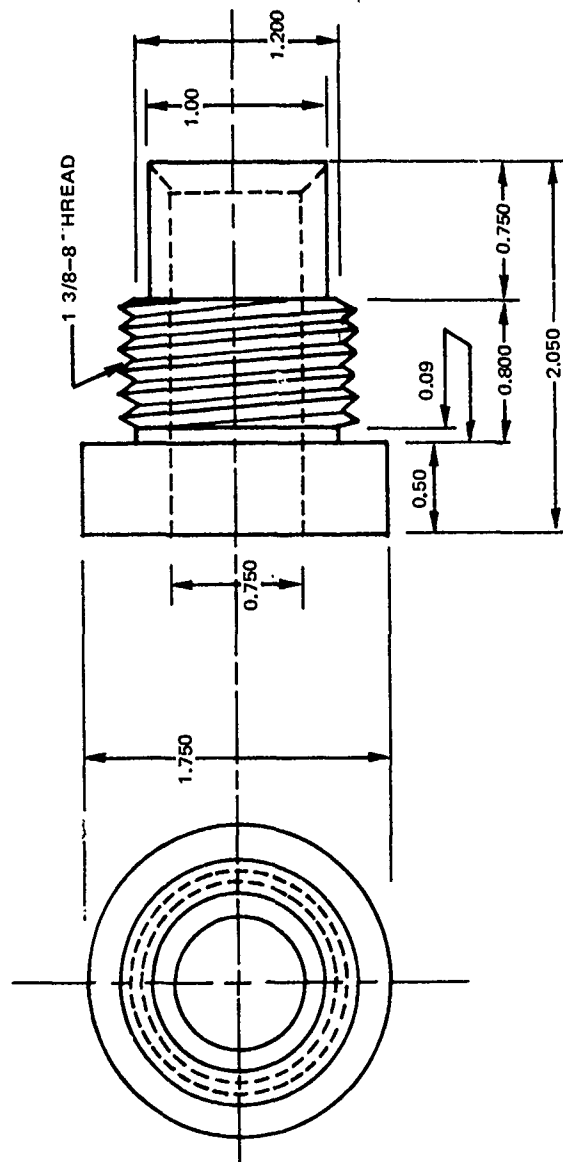


KEY

- A - GLASS REFERENCE ELECTRODE
- B - TEFLON ELECTRODE HOLDERS WITH O-RING SEALS
- C - TEFLON HOLDER FOR TEST SPECIMEN (WORKING ELECTRODE)
- D - TEST SPECIMEN
- E - LUGGEN PROBE (IR-FREE CONNECTOR TO REFERENCE ELECTRODE)
- F - LEAD TO TEST SPECIMEN
- G - GAS EXIT

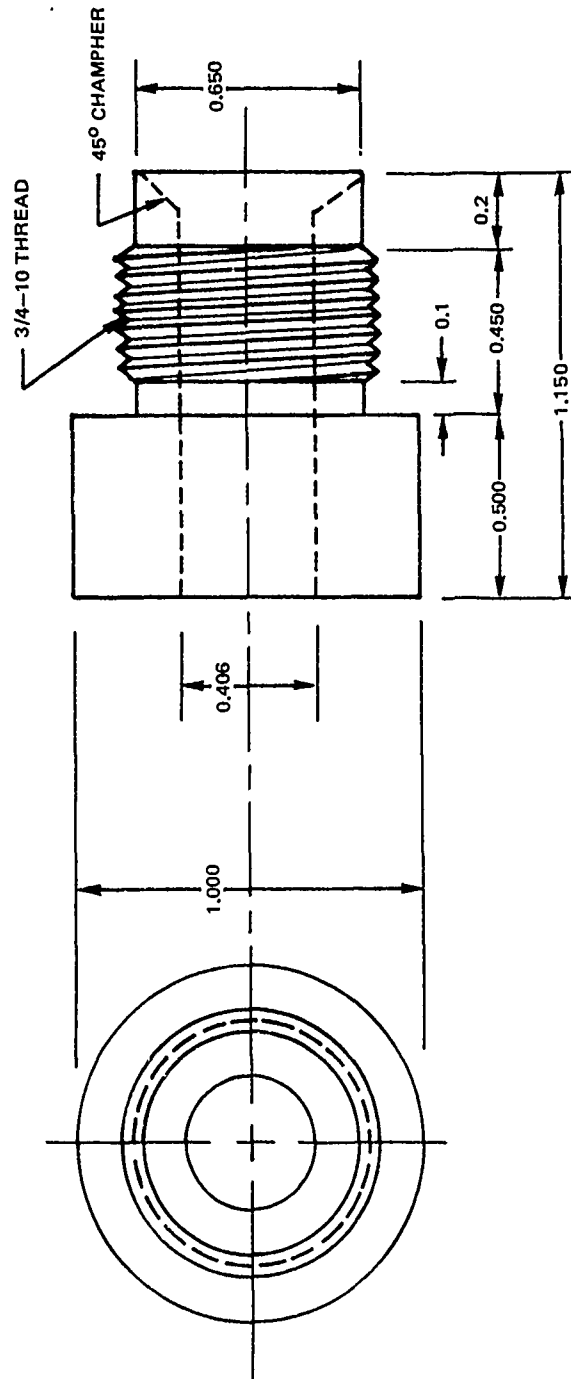
N08-56-1

THREADED TEFLON CAP
(25 mm)



MATERIAL: TEFLON
TOLERANCE: ±0.010
SCALE = FULL
ALL DIMENSIONS IN INCHES

THREADED TEFLON CAP
(15 mm)



MATERIAL : TEFLON

TOLERANCE : ± 0.010

SCALE = 1:2

ALL DIMENSIONS IN INCHES

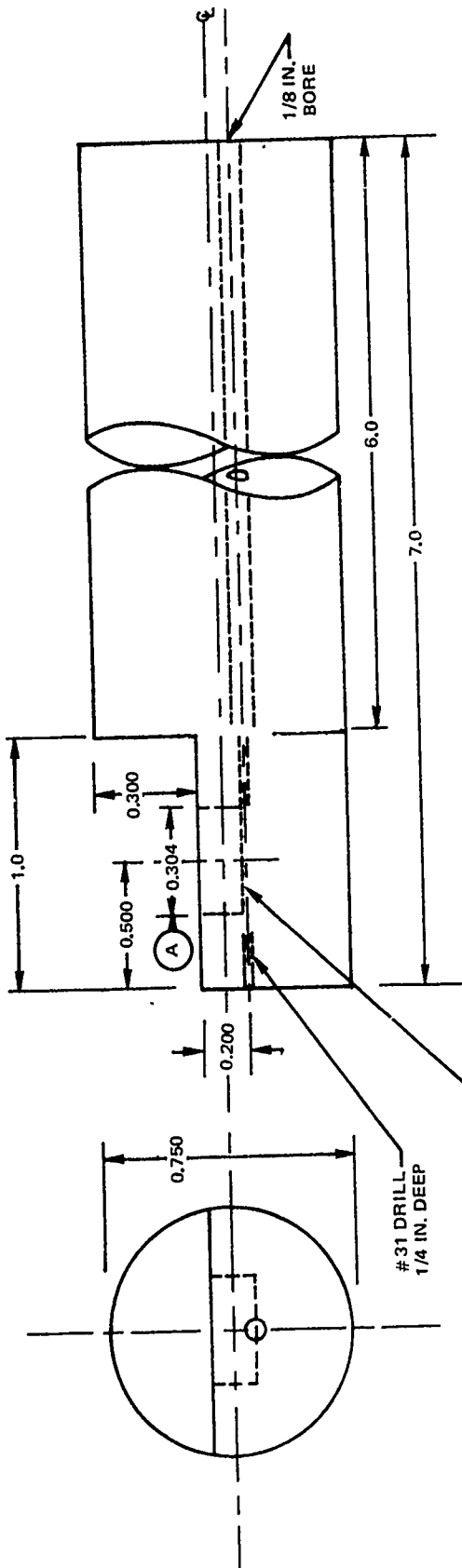
ELECTRODE HOLDER

MAT'L: TEFLON

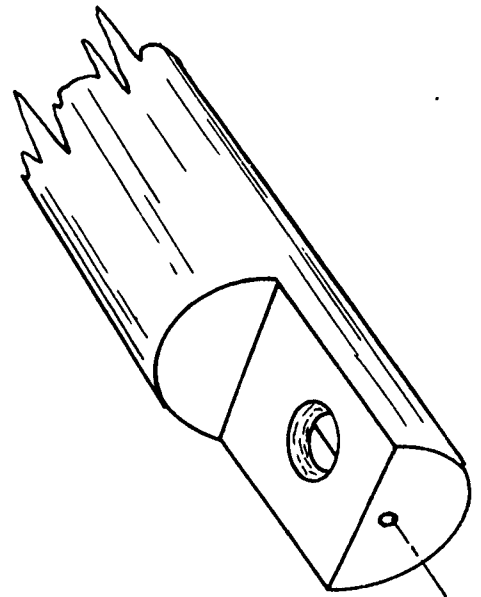
TOLERANCE: ± 0.010

SCALE: 1:2

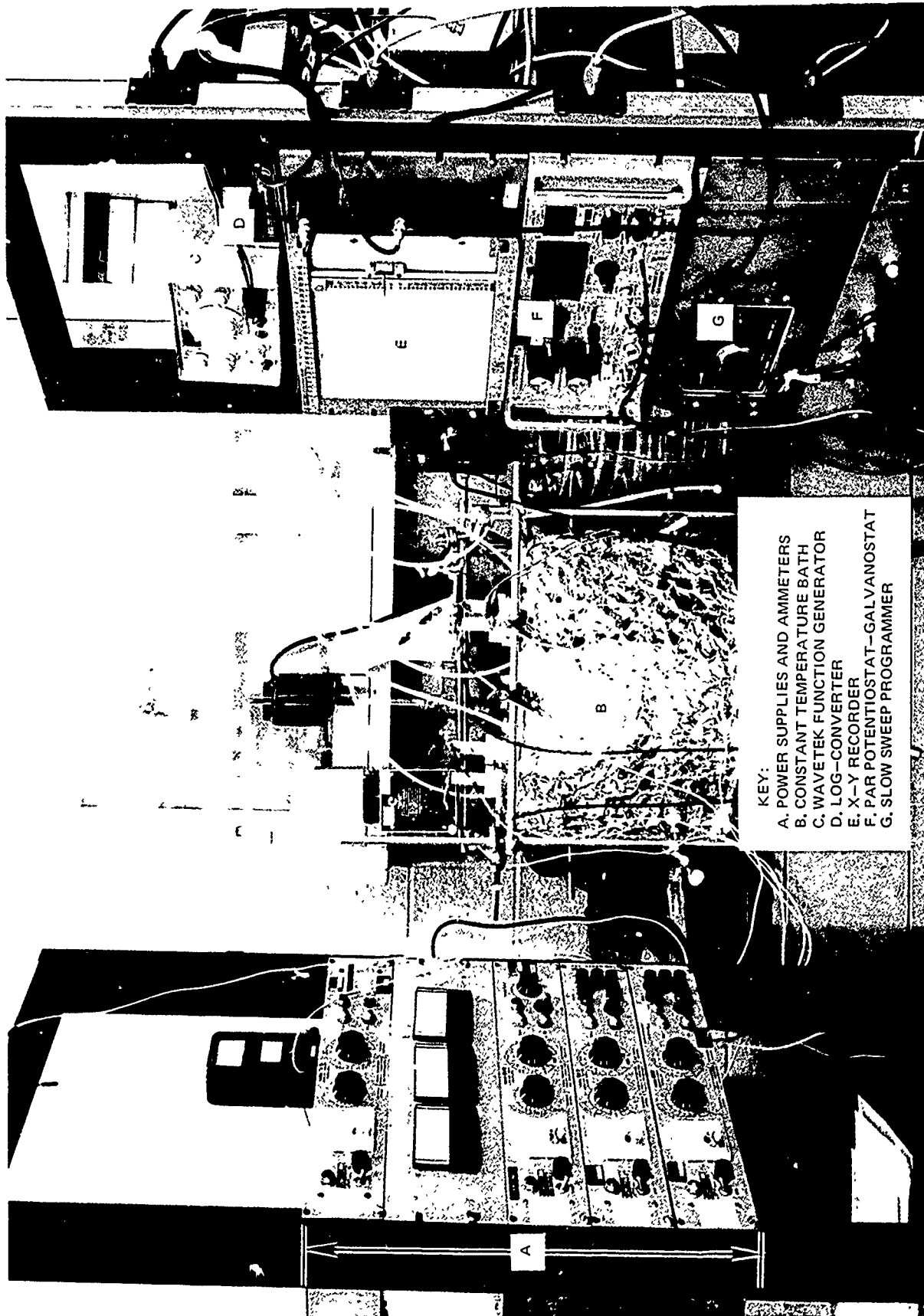
ALL DIMENSIONS IN INCHES



NOTE: (A) MUST BE HELD TO
 $+0.0010$ AND -0.002



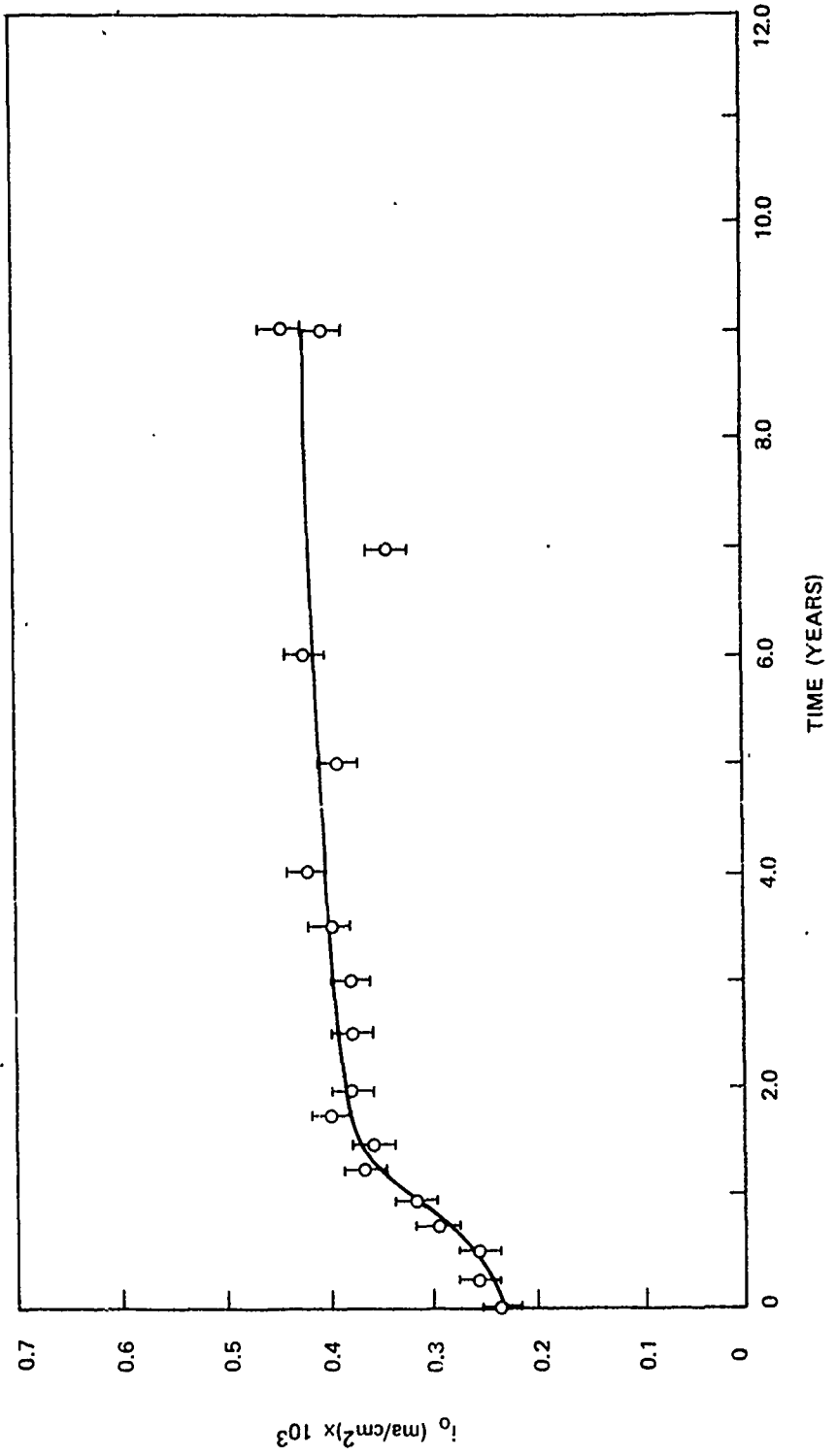
ELECTROCHEMICAL CORROSION TESTING APPARATUS



KEY:
A. POWER SUPPLIES AND AMMETERS
B. CONSTANT TEMPERATURE BATH
C. WAVETEK FUNCTION GENERATOR
D. LOG-CONVERTER
E. X-Y RECORDER
F. PAR POTENTIOSTAT-GALVANOSTAT
G. SLOW SWEEP PROGRAMMER

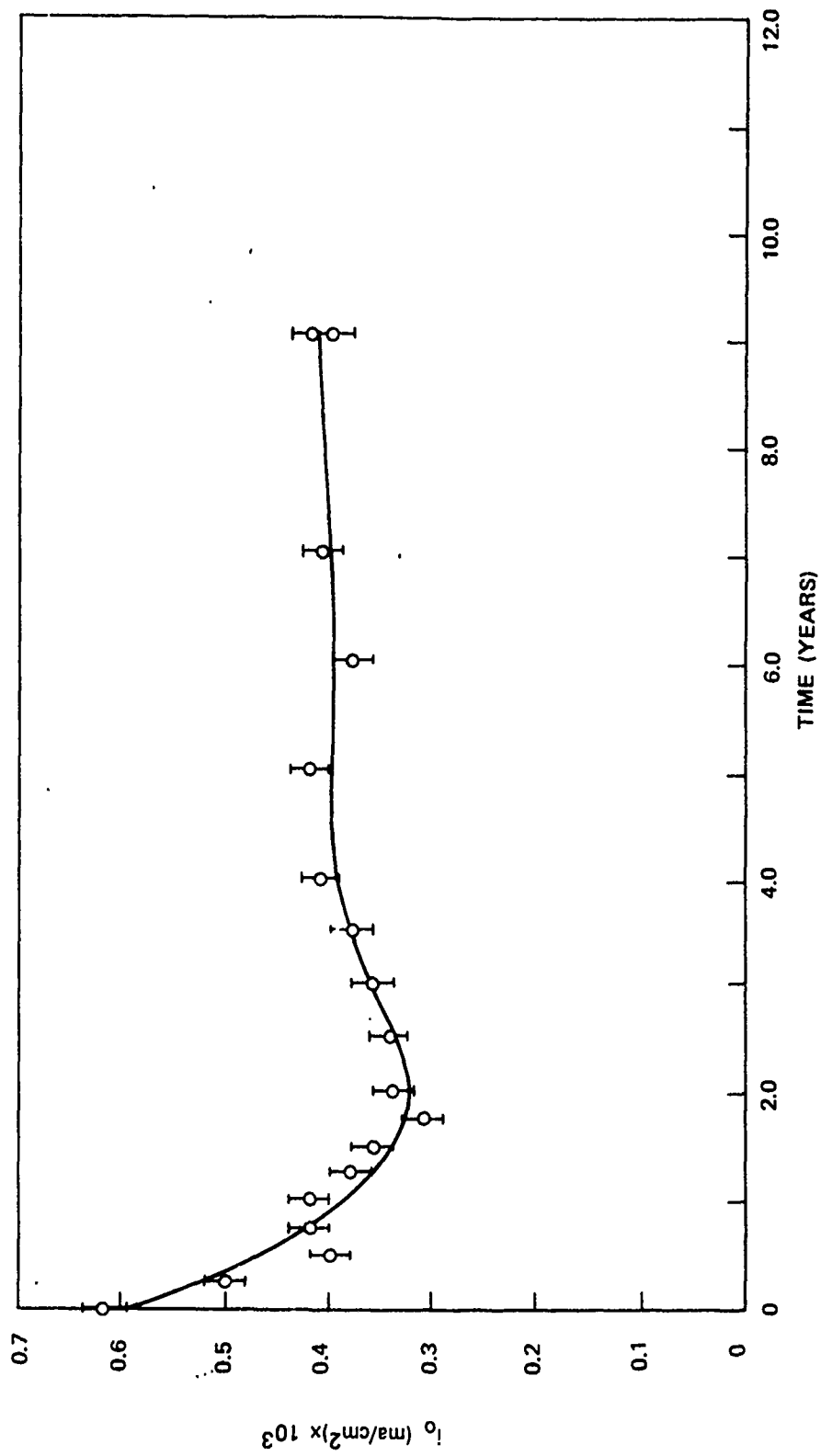
EQUILIBRIUM CORROSION CURRENT DENSITY (i_0) AS A FUNCTION OF ACCELERATED TIME

(Ti6Al4V AT 110°F)



EQUILIBRIUM CORROSION CURRENT DENSITY (i_o) AS A FUNCTION OF ACCELERATED TIME

(304L SS AT 110°F)



GRAECO-LATIN CUBE

FINAL i_0 (ma/cm²) x 10⁻³

MATERIAL 1

AA1100

TIME

		T ₁	T ₂	T ₃	T ₄
TEMPERATURE	R ₁	D _α 0.125	A _β 0.150	B _δ 0.090	C _γ 0.110
	R ₂	C _β 0.110	B _α 0.115	A _γ 0.165	D _δ 0.102
	R ₃	B _γ 0.115	C _δ 0.125	D _β 0.215	A _α 0.040
	R ₄	A _δ 0.110	D _γ 0.115	C _α 0.110	B _β 0.093

MATERIAL 2

AA6061-T6

TIME

		T ₁	T ₂	T ₃	T ₄
TEMPERATURE	R ₁	B _δ 0.075	C _γ 0.065	D _α 0.075	A _β 0.075
	R ₂	A _γ 0.070	D _δ 0.075	C _β 0.095	B _α 0.060
	R ₃	D _β 0.075	A _α 0.075	B _γ 0.080	C _δ 0.070
	R ₄	C _α 0.075	B _β 0.070	A _δ 0.075	D _γ 0.075

MATERIAL 3

AM355

TIME

		T ₁	T ₂	T ₃	T ₄
TEMPERATURE	R ₁	A _β 0.415	B _δ 0.380	C _γ 0.430	D _α 0.480
	R ₂	B _α 0.400	A _γ 0.430	D _δ 0.395	C _β 0.565
	R ₃	C _δ 0.530	D _β 0.350	A _α 0.420	B _γ 0.405
	R ₄	D _γ 0.535	C _α 0.475	B _β 0.420	A _δ 0.535

MATERIAL 4

17-7PH

TIME

		T ₁	T ₂	T ₃	T ₄
TEMPERATURE	R ₁	C _γ 0.430	D _α 0.445	A _β 0.435	B _δ 0.750
	R ₂	D _δ 0.275	C _β 0.390	B _α 0.300	A _γ 0.400
	R ₃	A _α 0.495	B _γ 0.345	C _δ 0.380	D _β 0.360
	R ₄	B _β 0.325	A _δ 0.585	D _γ 0.430	C _α 0.525

GRAECO-LATIN CUBE

FINAL i_0 (ma/cm²) x 10⁻³

MATERIAL 5
430SS
TIME

	T ₁	T ₂	T ₃	T ₄
R ₁	D _α 0.500	A _β 0.230	B _δ 0.425	C _γ 0.320
R ₂	C _β 0.540	B _α 0.420	A _γ 0.295	D _δ 0.700
R ₃	B _γ 0.280	C _δ 0.310	D _β 0.380	A _α 0.325
R ₄	A _δ 0.100	D _γ 0.425	C _α 0.700	B _β 0.620

MATERIAL 6
316LSS
TIME

	T ₁	T ₂	T ₃	T ₄
R ₁	B _δ 0.350	C _γ 0.455	D _α 0.395	A _β 0.420
R ₂	A _γ 0.115	D _δ 0.325	C _β 0.355	B _α 0.405
R ₃	D _β 0.445	A _α 0.690	B _γ 0.465	C _δ 0.270
R ₄	C _α 0.550	B _β 0.580	A _δ 0.485	D _γ 0.620

MATERIAL 7
304L SS
TIME

	T ₁	T ₂	T ₃	T ₄
R ₁	A _β 0.175	B _δ 0.480	C _γ 0.270	D _α 0.445
R ₂	B _α 0.380	A _γ 0.155	D _δ 0.475	C _β 0.235
R ₃	C _δ 0.360	D _β 0.310	A _α 0.370	B _γ 0.390
R ₄	D _γ 0.350	C _α 0.455	B _β 0.400	A _δ 0.455

MATERIAL 8
Ti 6Al4V
TIME

	T ₁	T ₂	T ₃	T ₄
R ₁	C _γ 0.340	D _α 0.430	A _β 0.150	B _δ 0.240
R ₂	D _δ 0.560	C _β 0.535	B _α 0.420	A _γ 0.280
R ₃	A _α 0.180	B _γ 0.280	C _δ 0.495	D _β 0.580
R ₄	B _β 0.100	A _δ 0.520	D _γ 0.050	C _α 0.960

ANODIC TEST SPECIMENS

(160°F - 10.0 YEARS)



BEFORE TEST (x4.5)

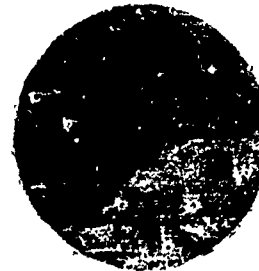


AFTER TEST (x4.5)

AA 1100
Cl IMPURITY
TRICHLOR AND
JOY CLEANING

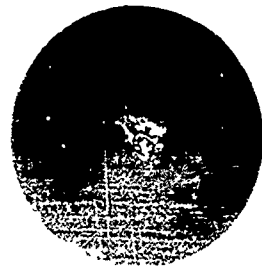


BEFORE TEST (x4.5)

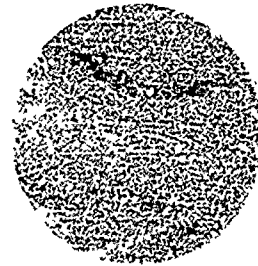


AFTER TEST (x4.5)

AA 6061 - T6
Zn IMPURITY
A CLEANING
PROCEDURE



BEFORE TEST (x4.5)



AFTER TEST (x4.5)

AM 355
CO₂ IMPURITY
B CLEANING
PROCEDURE



BEFORE TEST (x4.5)



AFTER TEST (x4.5)

17-7PH
H₂O IMPURITY
IPA AND JOY
CLEANING

76-03-219-2

ANODIC TEST SPECIMENS

(180°F- 10.0 YEARS)



BEFORE TEST (x4)

430 SS
Cl IMPURITY
TRICHLOR AND
JOY CLEANING

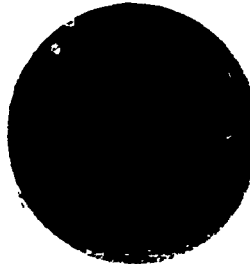


AFTER TEST (x4.5)

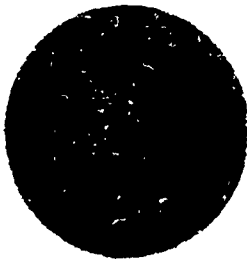


BEFORE TEST (x4.5)

316L SS
Zn IMPURITY
A CLEANING
PROCEDURE

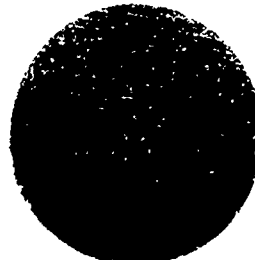


AFTER TEST (x4.5)



BEFORE TEST (x4)

304L SS
CO₂ IMPURITY
B CLEANING
PROCEDURE



AFTER TEST (x4.5)



BEFORE TEST (x4.5)

Ti6Al4V
H₂O IMPURITY
IPA AND JOY
CLEANING

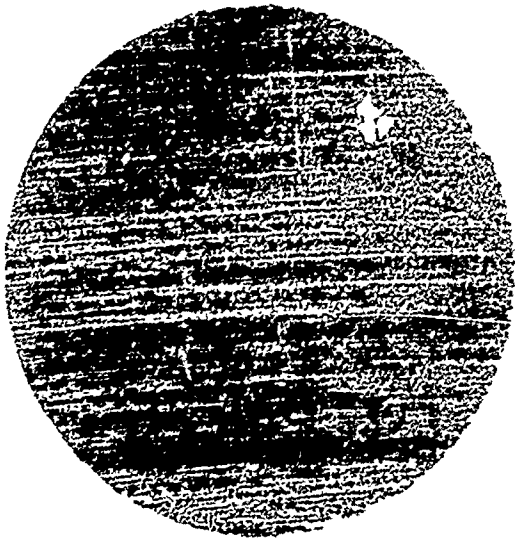


AFTER TEST (x4)

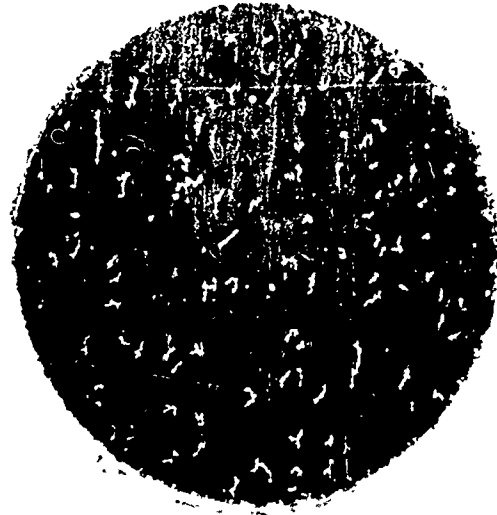
76-03-219-1

ANODIC TEST SPECIMENS

(Ti 6Al 4V)



BEFORE TEST (x9)



AFTER TEST (x8)

80° F; 4.0 YEARS; Cl IMPURITY
IPA AND JOY CLEANING



BEFORE TEST (x9)

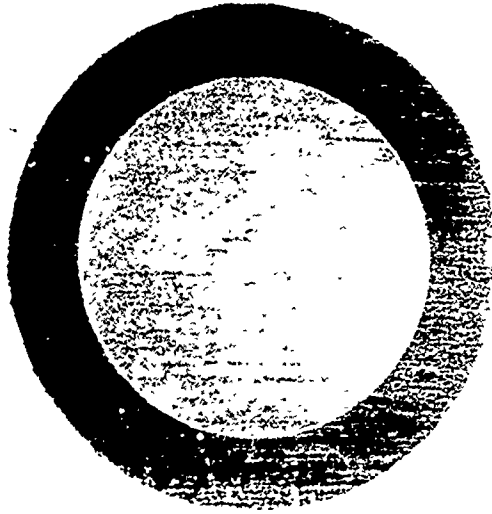


AFTER TEST (x9)

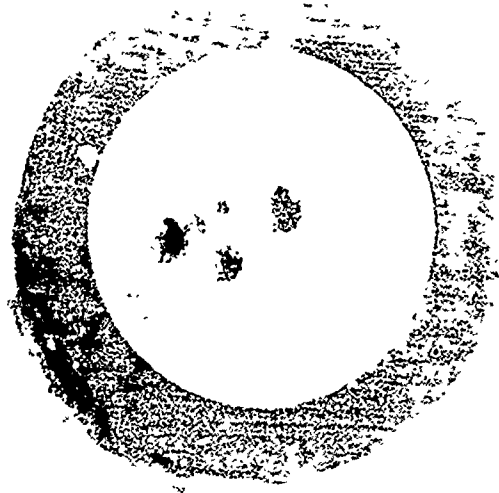
50° F; 1.0 YEAR; Zn IMPURITY
IPA AND JOY CLEANING

ANODIC TEST SPECIMENS

(BI-METALLIC*)
(160°F - 4.0 YEARS)

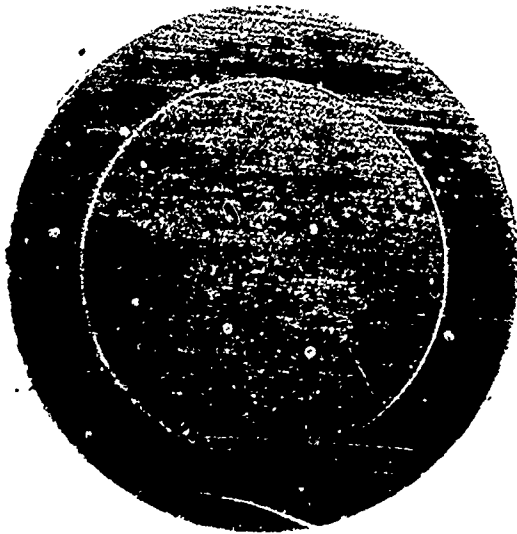


BEFORE TEST (x8)

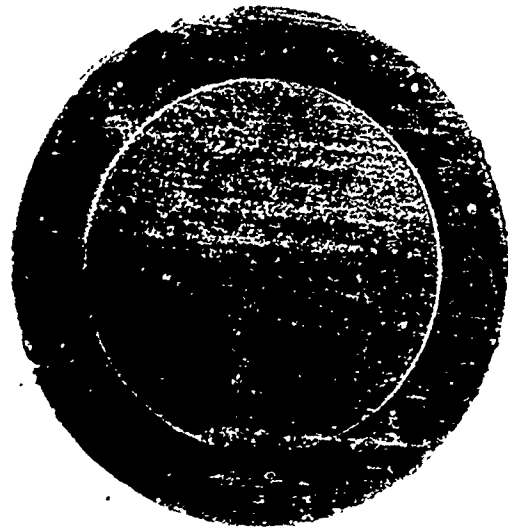


AFTER TEST (x8)

304L SS-AA6061-T6
Cl IMPURITY; IPA AND JOY CLEANING



BEFORE TEST (x9)



AFTER TEST (x9)

304L SS-Ti6Al 4V
CO₂ IMPURITY; TRICHLOR AND JOY CLEANING

*OUTER METAL IS 304L SS